SUPPLEMENTARY FIGURES FOR:

Molecular architecture, polar targeting and biogenesis of the *Legionella* Dot/Icm T4SS

Running title: Structural analysis of the *Legionella* T4SS

Debnath Ghosal[1,#], KwangCheol C. Jeong[2,3,#], Yi-Wei Chang[1,$], Jacob Gyore[2], Lin Teng[3], Adam Gardner[4], Joseph P. Vogel[2,*], Grant J. Jensen[1,5,*]

[1]Division of Biology and Biological Engineering,
California Institute of Technology,
Pasadena, CA 91125, USA.

[2]Department of Molecular Microbiology,
Washington University School of Medicine,
St. Louis, MO 63110, USA.

[3]Department of Animal Sciences &
Emerging Pathogens Institute,
University of Florida,
Gainesville, FL 32611, USA.

[4]Molecular Graphics Laboratory
Department of Integrative Structural
and Computational Biology
The Scripps Research Institute
La Jolla, CA 92037, USA.

[5]Howard Hughes Medical Institute,
California Institute of Technology,
Pasadena, CA 91125, USA.

#These authors contributed equally

[$]Current Address:
Departments of Biochemistry and Biophysics,
Perelman School of Medicine, University of Pennsylvania,
Philadelphia, PA 19104, USA.

[*]To whom correspondence should be addressed.
Email: jensen@caltech.edu and jvogel@wustl.edu

Lead contact: jensen@caltech.edu

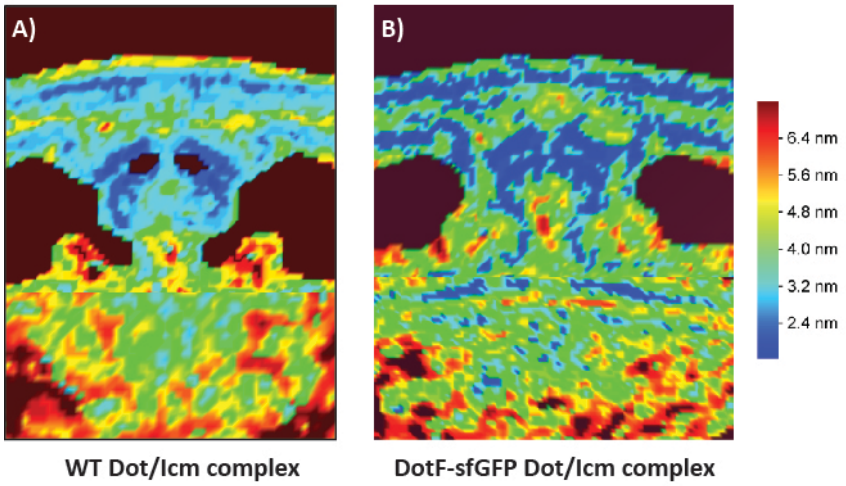

Supplementary Figure 1. Local resolution of subtomogram averages. (A) WT Dot/Icm complex, (B) DotF-sfGFP stabilized Dot/Icm complex. Local resolutions are calculated by ResMap[1].

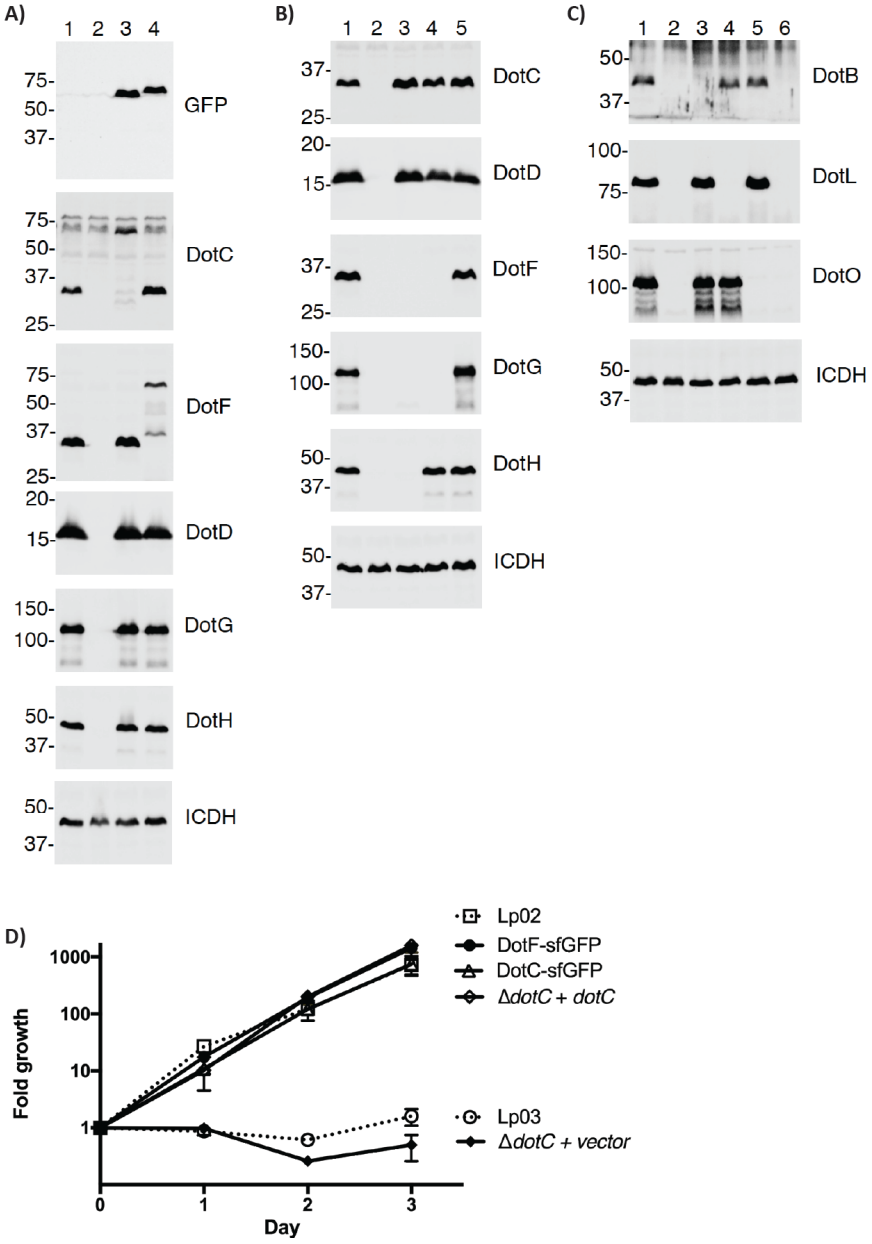

Supplementary Figure 2. Confirmation of *L. pneumophila* strains. Western blots with the indicated Dot-specific antibodies. Isocitrate dehydrogenase (ICDH), a cytoplasmic house-keeping protein, was used as a loading control for each set of blots. Samples were loaded in the following order: (A) 1. Lp02 (wild-type), 2. JV5319 (SΔ(UF)), 3. JV9114 (DotC-sfGFP), 4. JV9082 (DotF-sfGFP), (B) 1. Lp02 (wild-type), 2. JV5319 (SΔ(UF*)*), 3. JV7058 (Δ*dotF* Δ*dotG* Δ*dotH*), 4. JV5460 (SΔ(UF*)* + DotCDH), 5. JV5443 (SΔ(UF*)* +DotCDFGH), and (C) 1. Lp02 (wild-type), 2. JV5319 (SΔ(UF*)*), 3. JV918 (Δ*dotB*), 4. JV2422 (Δ*dotA* Δ*dotL*), 5. JV1644 (Δ*dotO*), 6. JV6781 (Δ*dotB* Δ*dotL* Δ*dotO*). Similar blots are already published for other mutants[2-5]. Each of these experiments were done three times and representative blots are shown. (D) Strains expressing DotF-sfGFP and DotC-sfGFP are functional for intracellular growth. A wild-type *Legionella* strain (Lp02), a strain expressing DotF-sfGFP (JV9082), a strain expressing DotC-sfGFP (JV9114), a Δ*dotC* mutant containing wild type *dotC* (JV5264), a T4SS-defective strain with a *dotA* mutation (Lp03), or a Δ*dotC* mutant containing vector (JV5263) were used to infect U937 cells. Growth was assayed by plating for colony forming units (CFUs) over three days. Data is representative of three independent experiments.

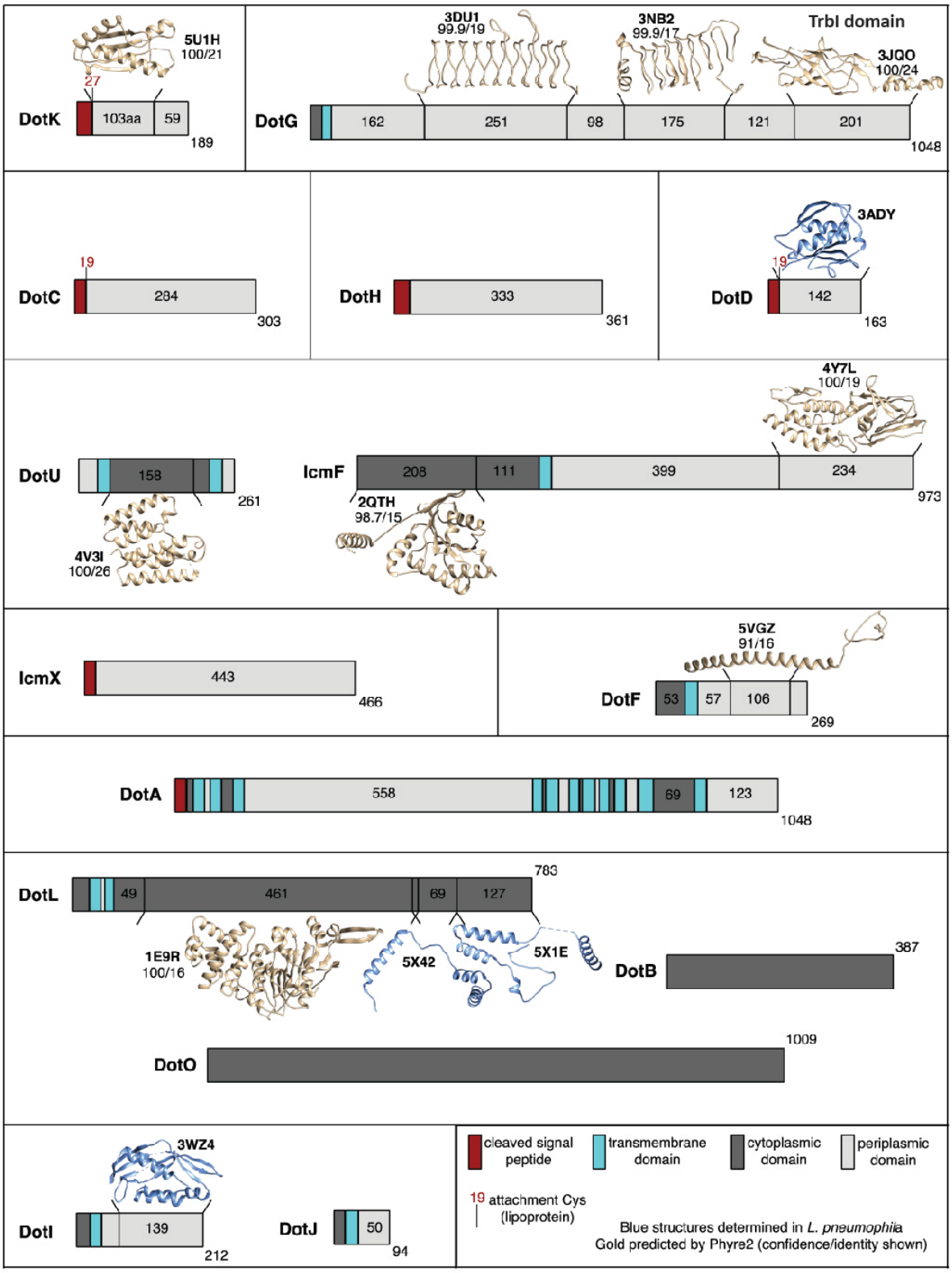

Supplementary Figure 3. Domain structures of proteins considered here. (see legend on next page)

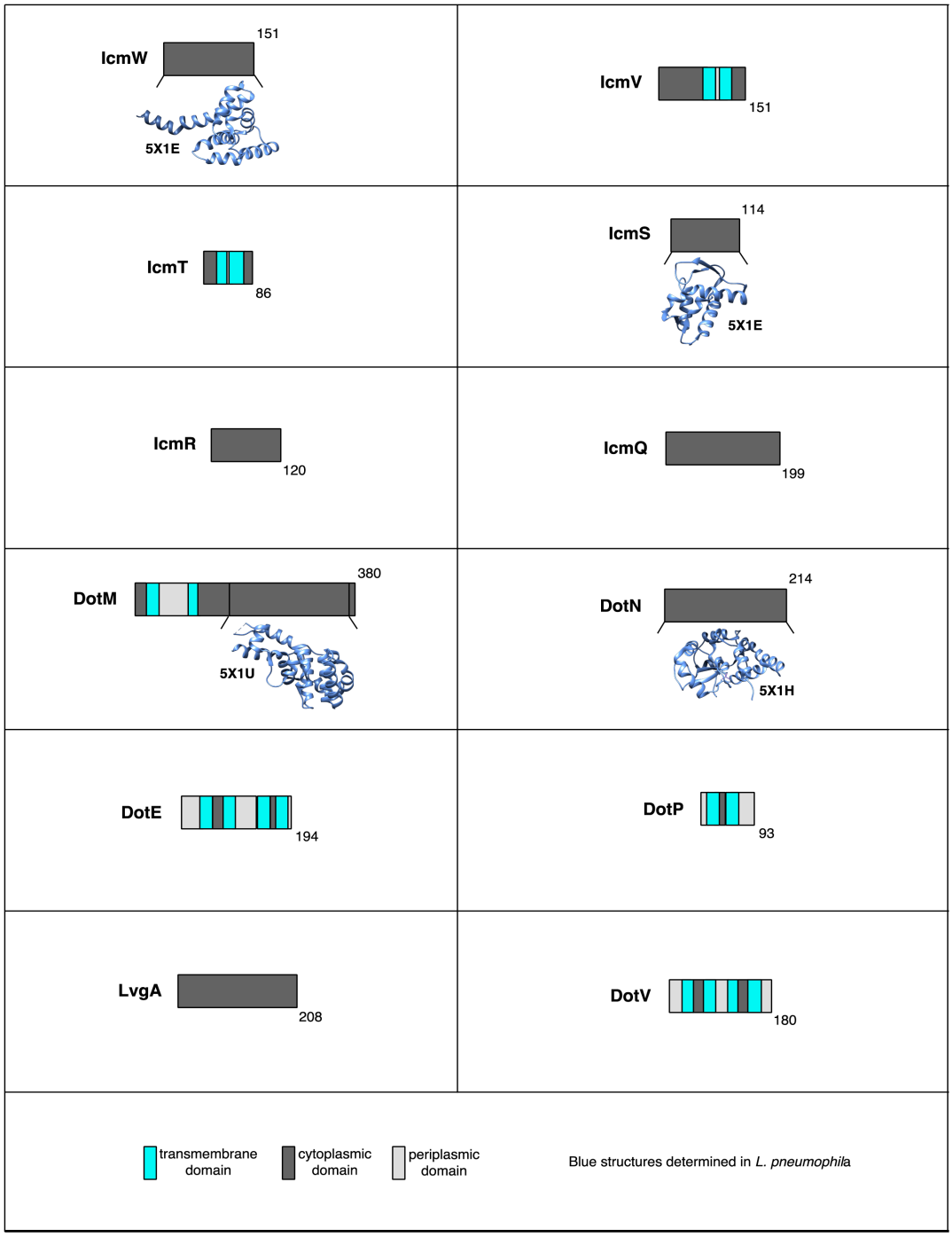

Supplementary Figure 4. Domain structures of components not treated in this study. Sequences of different proteins obtained from UniProt. Predicted domains (by Phyre2[6], I-TASSER[7] and Quark[8]) are shown from N- (left) to C-terminus (right). Red = cleaved signal peptide, cyan = transmembrane domain (TMHMM/Phobius), dark gray = cytoplasmic domain, light gray = periplasmic domain. Domains whose structure has been solved (blue) or predicted with high confidence (gold) are indicated. In each case, the structure (with PDB ID, and confidence/sequence identity for Phyre2 predictions) is shown above the domain if periplasmic and below if cytoplasmic. The length of key domains is indicated, with total protein length listed at the C-terminus. The locations of cysteines in lipoproteins (SignalP 4.1) that are linked to the OM are noted in red.

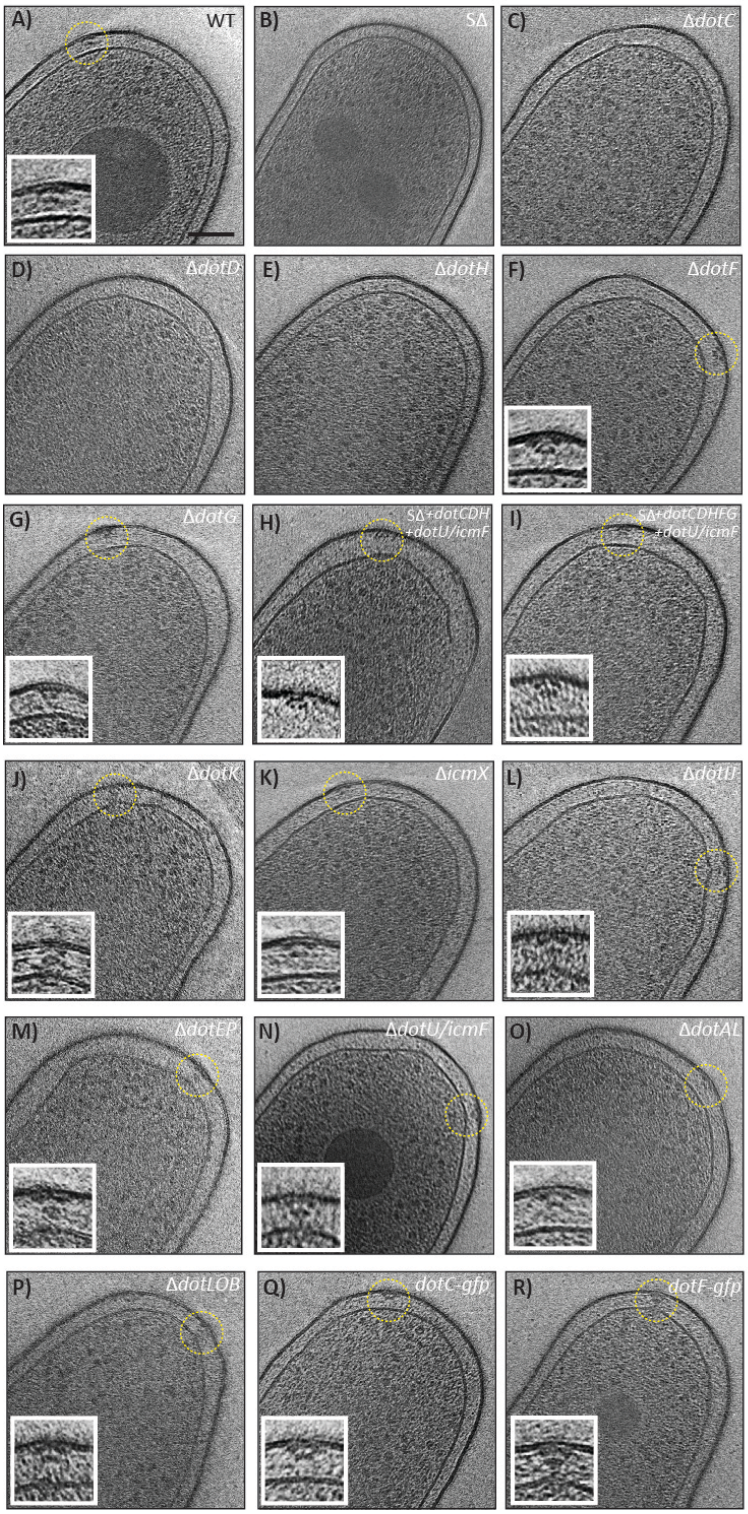

Supplementary Figure 5. Electron cryotomography of intact *Legionella pneumophila* cells expressing T4SSs. (A-R) Panels show tomographic slices 8-nm thick through one representative cell of each strain imaged. The strain identity is given in the upper right corner of each panel. In those strains in which T4SS particles or sub-particles were seen, an enlarged image of an example particle is shown in the inset. Scale bar (A-R) 100 nm.

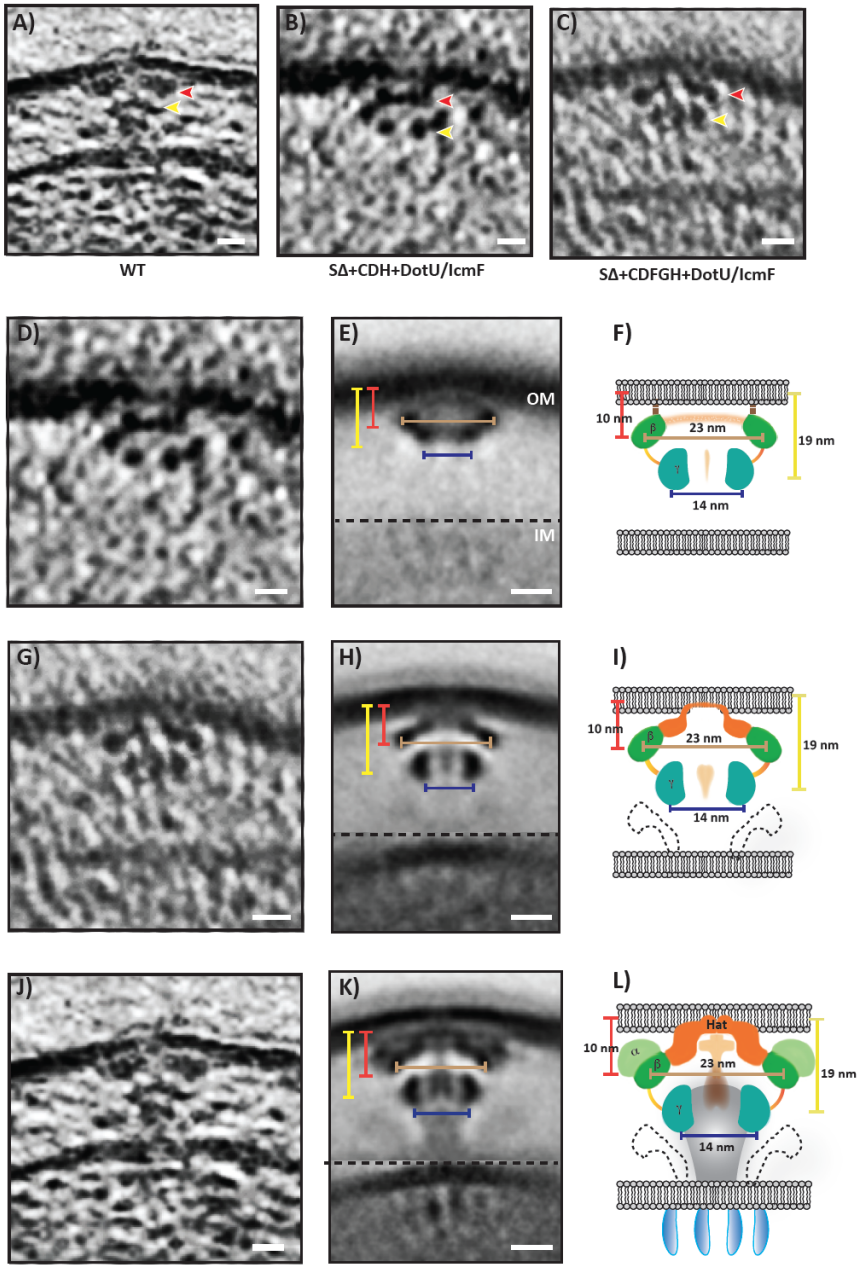

Supplementary Figure 6. Beta and gamma densities are present in WT, reconstituted DotCDH (+DotU/IcmF) and reconstituted DotCDHFG (+DotU/IcmF) complexes. (A-C) Gamma densities in individual particles of the reconstituted DotCDH (+DotU/IcmF) complex are comparable to those of the reconstituted DotCDHFG (+DotU/IcmF) complex and the WT complex. However, due to flexibility, they appear less pronounced in the reconstituted DotCDH (+DotU/IcmF) average. Red arrowheads point to beta-densities and yellow arrowhead point to gamma densities. (D-F) Showing individual reconstituted DotCDH (+DotU/IcmF) subcomplex (D), subtomogram average of the DotCDH (+DotU/IcmF) subcomplex (E), and schematic of the reconstituted average (F) showing distances between the two beta-densities (beige, 23 nm), distance between the two gamma densities (dark blue, 14 nm) and the distance between the OM and the beta densities (red, 10 nm), and distance between the OM and the gamma densities (yellow, 19 nm). (G-I) Same as (D-F) but for the reconstituted DotCDHFG (+DotU/IcmF) core-complex. (J-L) Same as (D-F) but for the WT Dot/Icm T4BSS complex. Scale bar 10 nm (A-C,D,E,G,H,J,K). Number of tomograms and particles used for the subtomogram average are listed in Supplementary Information Table 1.

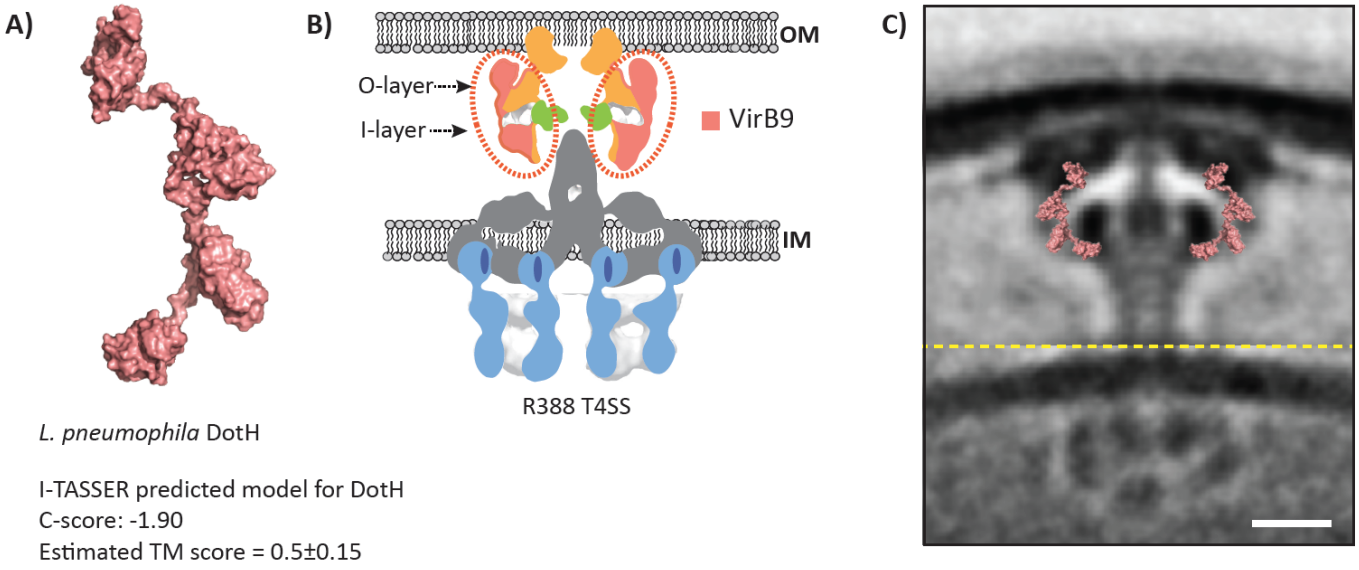

Supplementary Figure 7. Secondary structure predictions of DotH. (A) Prediction of DotH structure using I-TASSER suggests that DotH includes two or more separate domains. (B) DotH and VirB9 are suggested to be counterparts. VirB9 in the T4ASS also has two separate domains that extend between the O-layer and the I-layer[9]. (C) DotH's predicted structure fits well in the Dot/Icm complex. Circumstantial evidence suggests that DotH would extend between the beta and the gamma densities along the elbow very much like VirB9. Scale bar 10 nm (C).

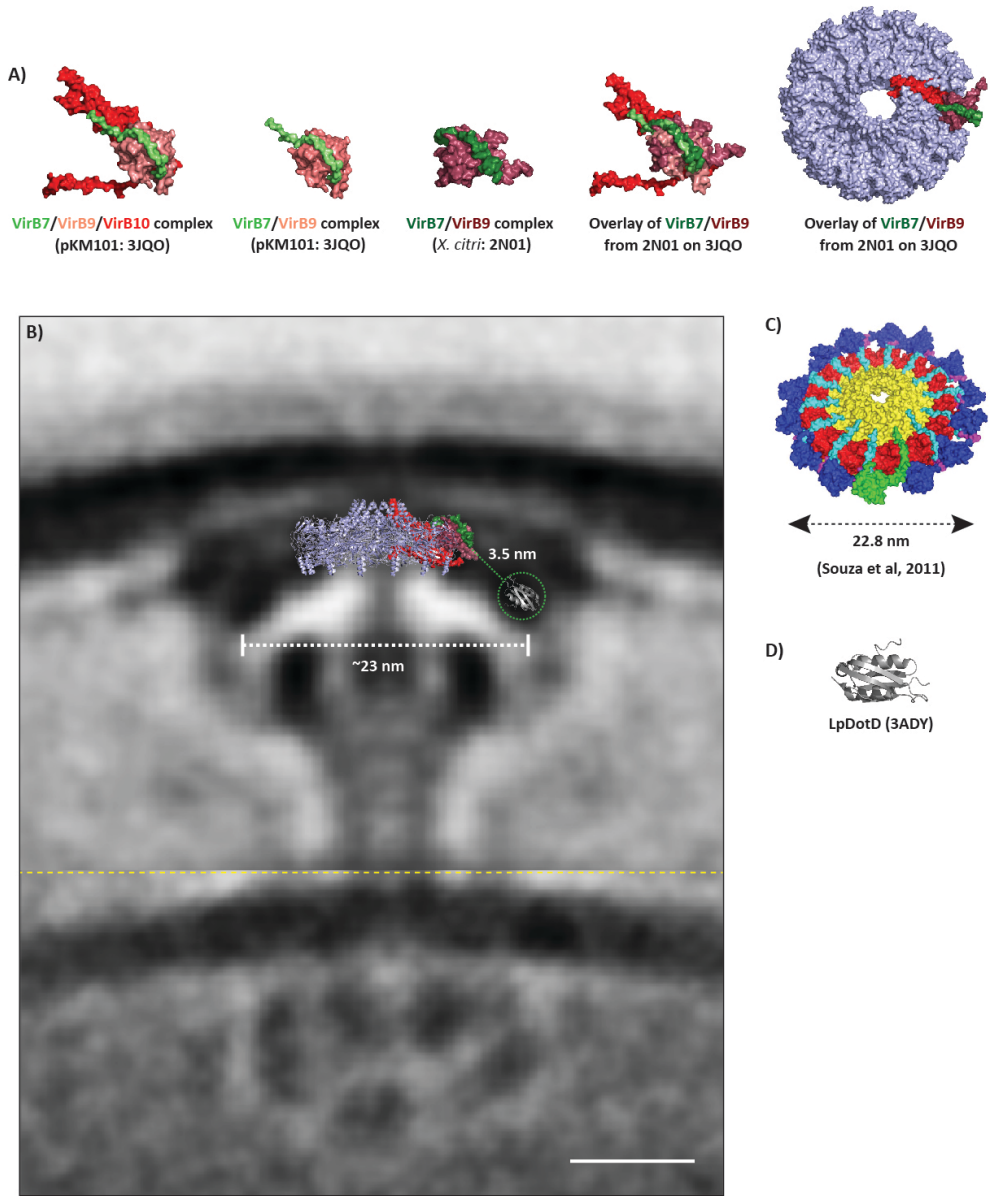

Supplementary Figure 8. Positioning of DotD's N0 domain. (A-B) Overlaying the *X. citri* VirB7/9 complex (2N01) on the pKM101 VirB7/9/10 OM complex (3JQO) indicates that the *X. citri* VirB7-N0 domain would be at the periphery of the OM complex. Since VirB7 and DotD are counterparts and DotD also has an N0 domain, we propose that DotD's N0 domain would occupy a very similar position as *X. citri* VirB7's N0 domain. Comparing the lipidation residue, and length of DotD's N-terminal disordered region and *X. citri* VirB7/VirB9 interaction interface, we propose that DotD's N0 domain will be 3.5 nm or less away from the hat. The only unaccounted-for density within that distance from the periphery of the hat is the beta density. The beta densities form a ring of diameter ~23 nm. (C) A very similar diameter ring was proposed by Souza et al. for the *X. citri* VirB7-N0 domain. (D) Crystal structure of the *L. pneumophila* DotD N0 domain. Scale bar 10 nm (B).

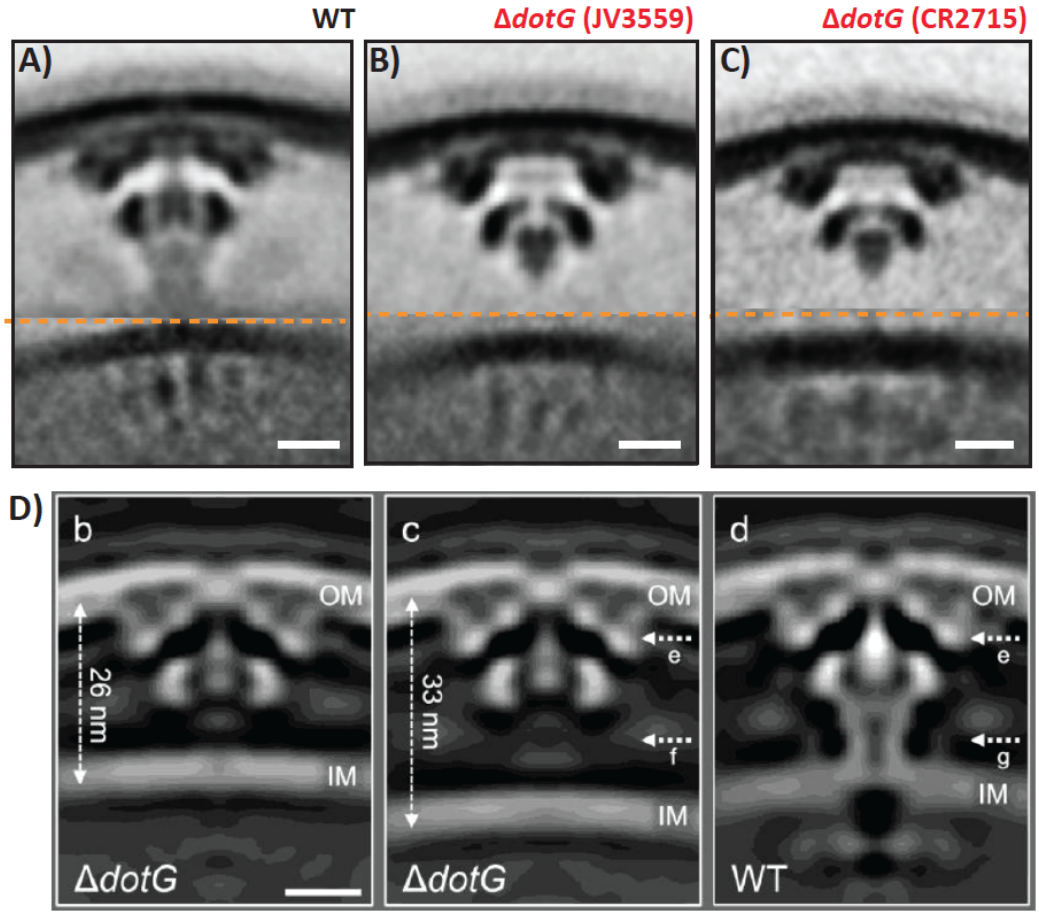

Supplementary Figure 9. Discrepancies between the subtomogram averages of a Δ*dotG* mutant. Previously a subtomogram average was reported for the Δ*dotG* mutant strain CR2715[10], which was constructed in the Roy laboratory (Yale University). However, the average was substantially different than what was observed using an independently constructed Δ*dotG* strain, JV3559 (Vincent et al, 2006). To resolve this difference, CR2715 was reimaged using the same technique as done for JV3559. (A-C) Central slices through sub-tomogram averages of the (A) WT Dot/Icm complex, (B) the Δ*dotG* average from the JV3559 strain used in this study, and (C) the Δ*dotG* average from the CR2715 strain used by Chetrit et al. In our hands, both Δ*dotG* strains (JV3559 and CR2715) produced identical results as including the absence of the OM associated "hat" structure, a lowered "plug" density and the disappearance of the stalk-channel. In contrast, Chetrit et al reported no changes in the "hat" and "plug" density but observed alteration in the stalk-channel density[10]. Based on our analysis, the Δ*dotG* subtomogram averages reported in Chetrit et al are more consistent with the absence of *dotA* (Fig. 2Q, 2U). (D) Central slice through sub-tomogram averages of Δ*dotG* complex (b-c) (reproduced from Chetrit et al[10], b-c represent two different classes); the WT complex is shown in panel d). (A-D) Scale bar 10 nm.

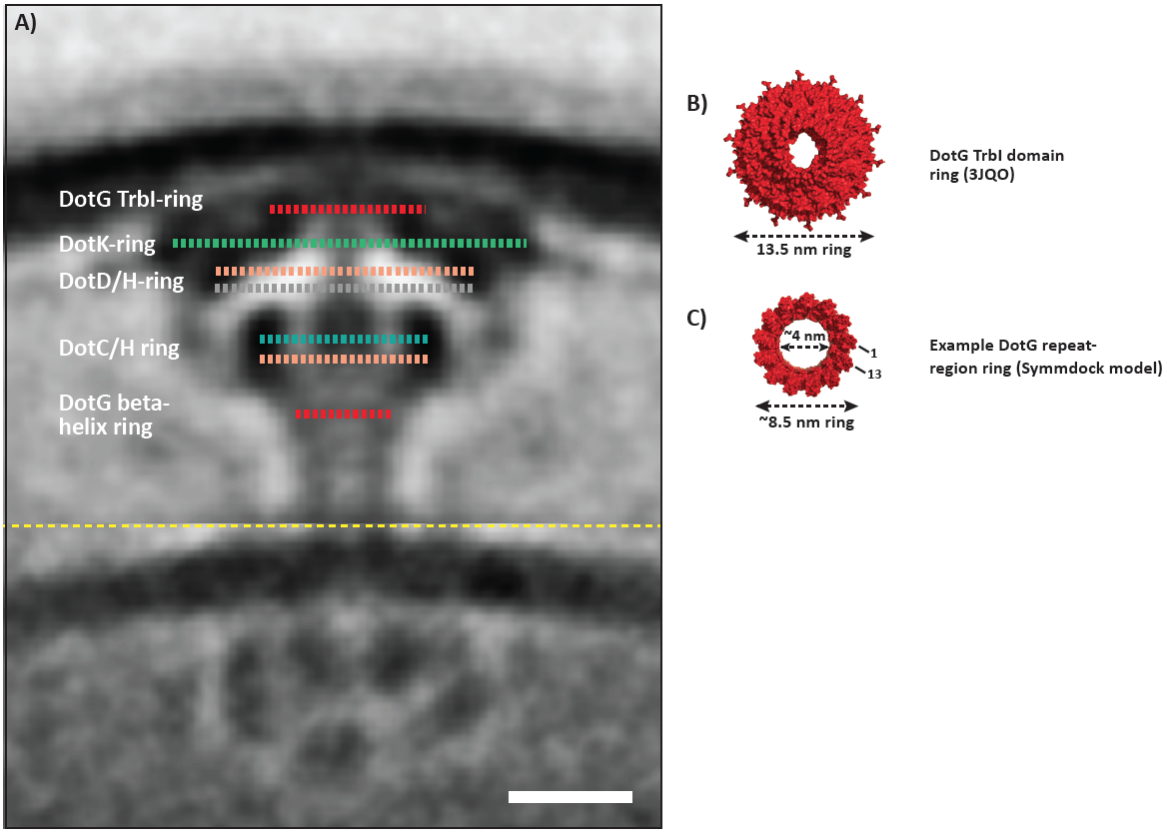

Supplementary Figure 10. The Dot/Icm complex is composed of several stacked ring-like structures. (A) OM-associated DotG TrbI-ring (red dotted line), DotK-ring (green dotted line), DotD/H-ring (salmon and grey dotted lines), periplasmic DotC/H-ring (cyan and salmon dotted lines), and DotG beta-helix ring (red dotted line). (B) A top-view of the TrbI ring formed by VirB10 in the VirB7/9/10 complex (3JQO). (C) Cross-section of the periplasmic channel formed by the DotG repeat region with an inner lumen diameter of ~4 nm and an outer diameter of ~8.5 nm. Outer and inner diameters of a 13-mer ring are consistent with the channel width seen in the subtomogram average. Scale bar 10 nm (A).

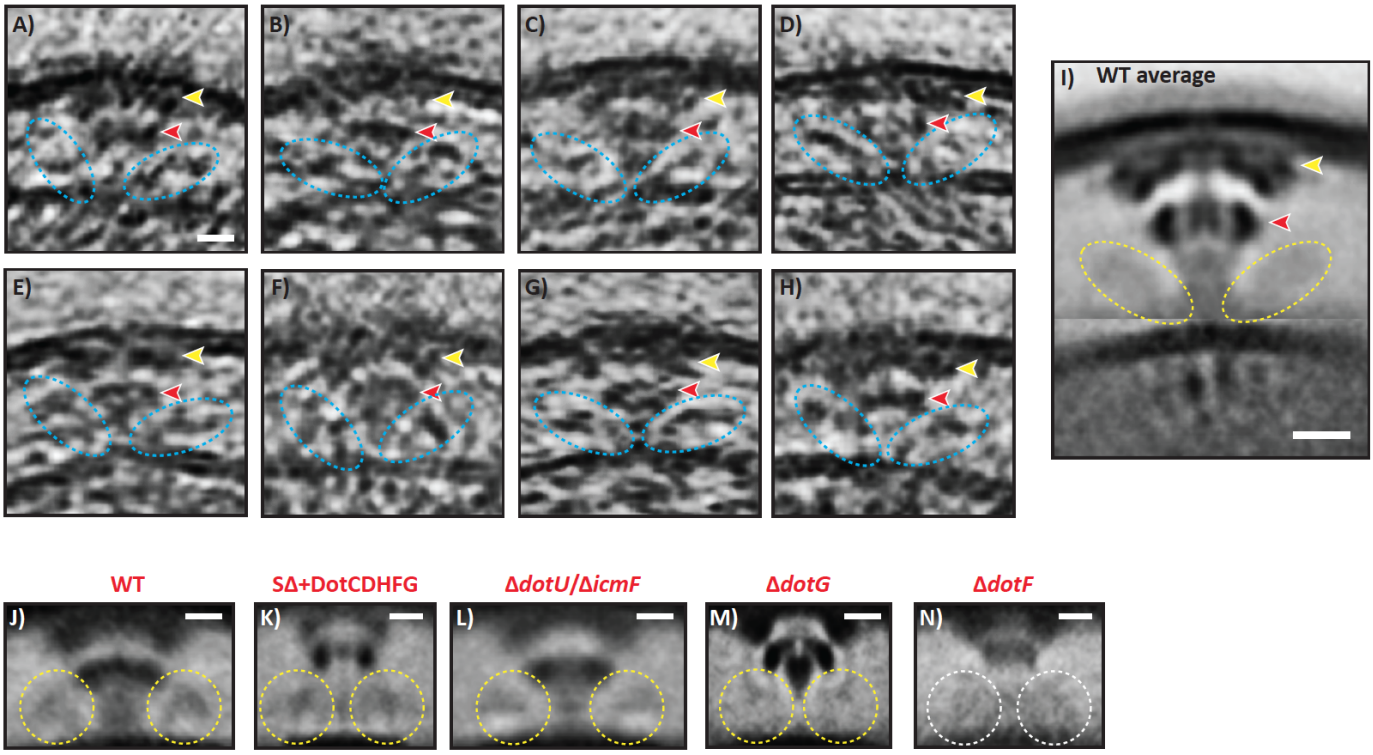

Supplementary Figure 11. Flexibility and identification of the wings as DotF. (A-H) Tomographic slices through wild-type T4BSSs showing wing densities (circled in blue) in various locations with respect to the membranes and the rest of the T4BSS. (I) Average of the wild-type T4BSS, with yellow and red arrowheads and yellow circles as in individual particles for positional reference. Scale bar 10 nm. (J-N) Central slices through sub-tomogram averages of various strains with particles aligned on the region of the wing density (between IM and gamma ring). Yellow circles indicate presence of wings, white circles indicate absence. Scale bar 10 nm (A-N).

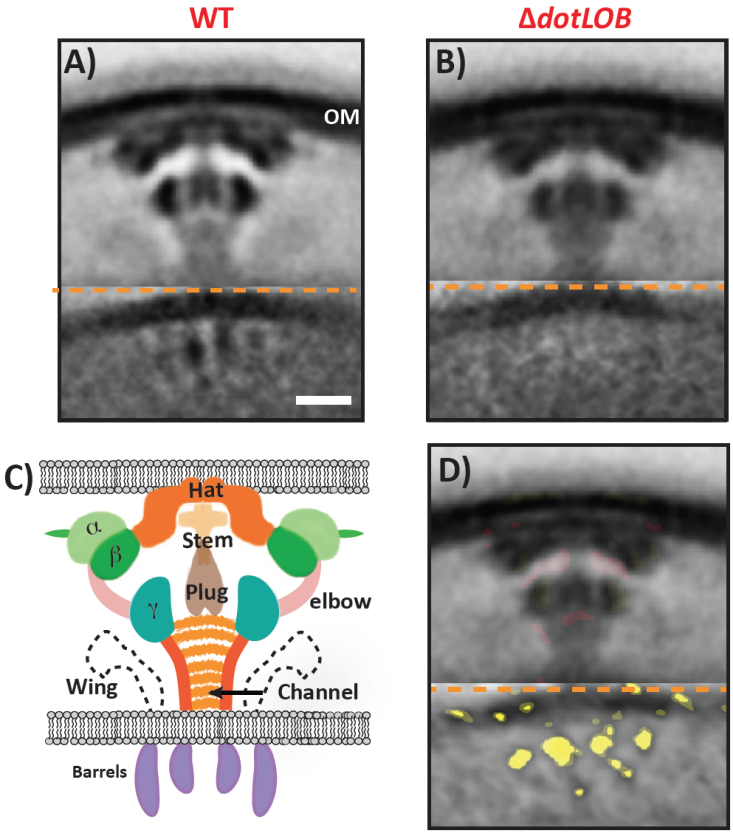

Supplementary Figure 12. Cytoplasmic densities are missing due to the loss of the DotL, DotO, DotB (DotLOB) ATPases. Central slices through the sub-tomogram average structures of the WT Dot/Icm T4BSS (A) and a mutant strain lacking the DotLOB ATPases (B). (C) Schematic of the WT complex showing distinct densities. Cytoplasmic densities are shown in purple. (D) Difference map between the WT structure and the ATPase deletion structure. Yellow represents missing densities and red extra densities. Weak to strong intensities correspond to density differences from one to three standard deviations, respectively, overlaid on the mutant sub-tomogram average. In the deletion mutant all the cytoplasmic densities are missing. Scale bar 10 nm (A,B,D).

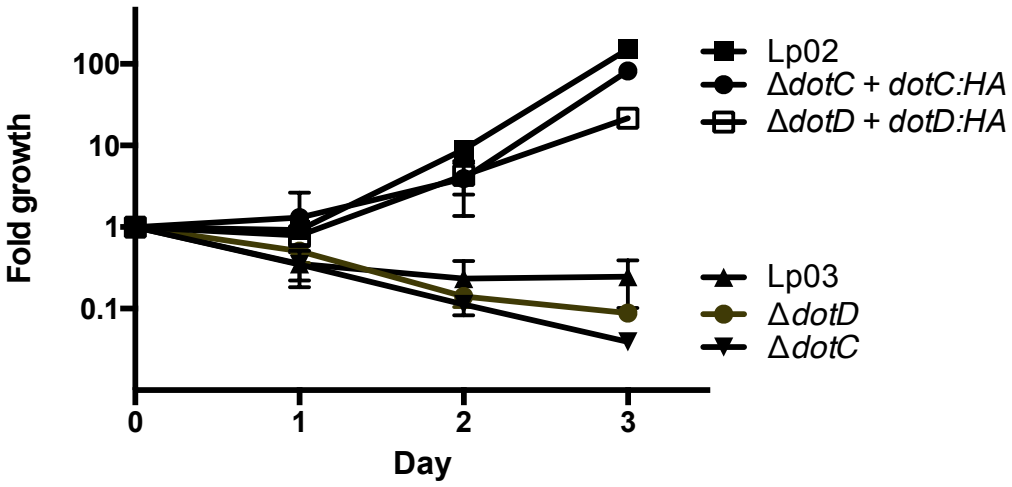

Supplementary Figure 13. Epitope tagged versions of DotC and DotD are functional for intracellular growth. DotC and DotD were fused to the HA tag at their C-termini and expressed in a Δ*dotC* mutant and a Δ*dotD* mutant, respectively. A wild type *Legionella* strain (Lp02), a *dotA* mutant (Lp03), a Δ*dotC* mutant containing vector (JV5263) or wild type DotC (JV5264) or DotC-HA3X (JV5484) and a Δ*dotD* mutant containing vector (JV5266) or wild type DotD (JV5267) or DotD-HA3X (JV5268) were used to infect U937 cells. Growth was assayed by plating for colony forming units (CFUs) over three days. Data is representative of three independent experiments (n=3). Data are presented as means ± SEM.

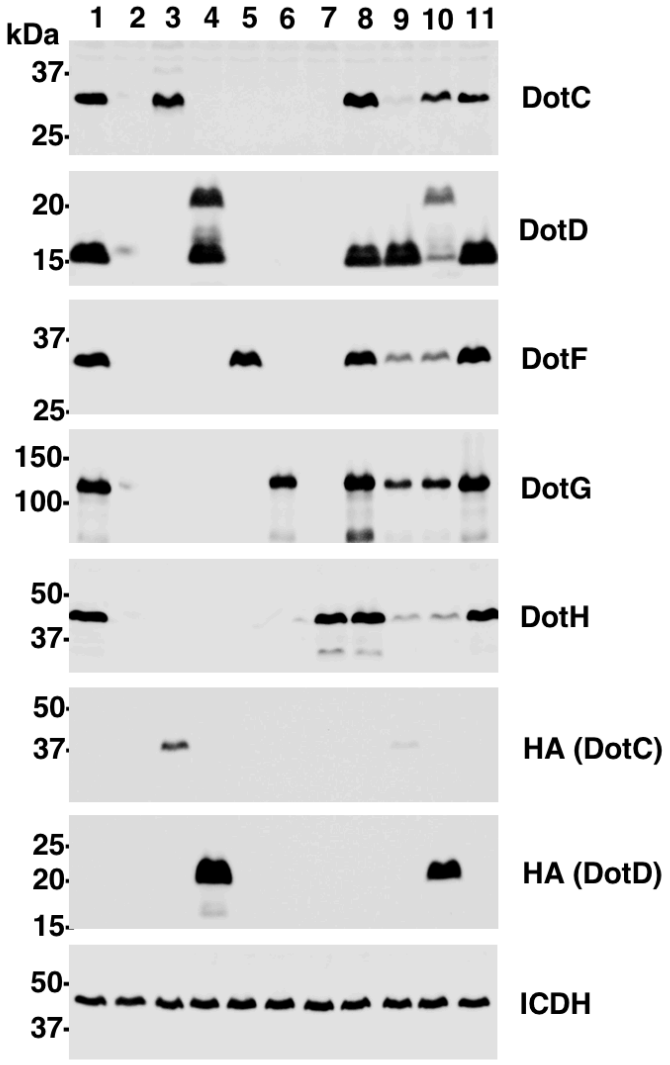

Supplementary Figure 14. Expression of the correct components in the SΔ strain (JV4044) for Figure 3A. *L. pneumophila* strains were grown to late exponential phase and westerns were done with the indicated antibodies. Isocitrate dehydrogenase (ICDH), a cytoplasmic housekeeping protein, was used as a loading control. Samples were loaded in the following order: 1. JV1139 (Lp02 + pJB908), 2. JV4209 (SΔ + vector), 3. JV4694 (SΔ + *dotC:HA3x*), 4. JV4695 (SΔ + *dotD:HA3x*), 5. JV4669 (SΔ + *dotF*), 6. JV4688 (SΔ + *dotG*), 7. JV4671 (SΔ + *dotH*), 8. JV5442 (SΔ + *dotCDFGH*), 9. JV9128 (SΔ + *dotC:HA3x dotD dotFGH*), 10. JV9129 (SΔ + *dotD:HA3x dotC dotFGH*), 11. JV1139 (Lp02 + pJB908). Each of these experiments were done three times and representative blots are shown.

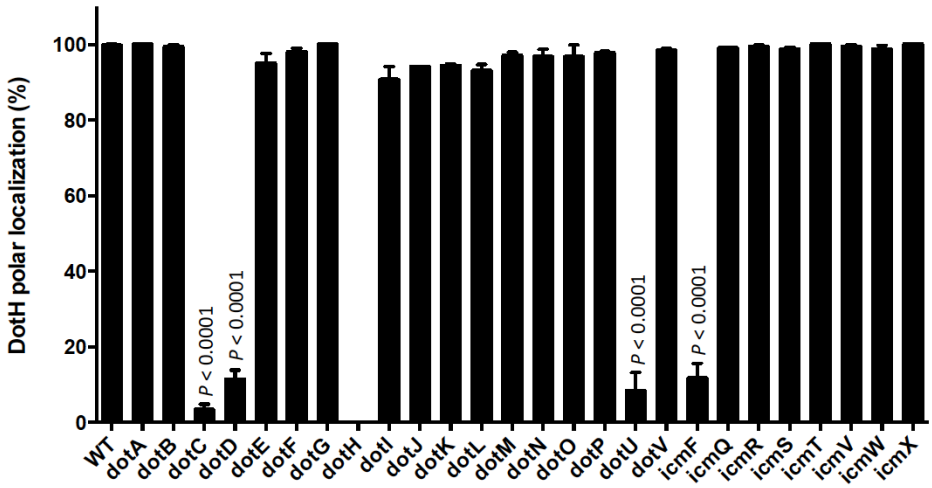

Supplementary Figure 15. Quantitation of polar localization of DotH for Figure 3B. The percent of cells having polar localization of the DotH in individual *dot/icm* deletions was determined from three independent experiments (n=3) (100 cells counted from each experiment). Data are presented as means ± SEM. P value indicates statistical difference compared to the wild-type strain Lp02 (WT) by unpaired two-tailed Student's t-test.

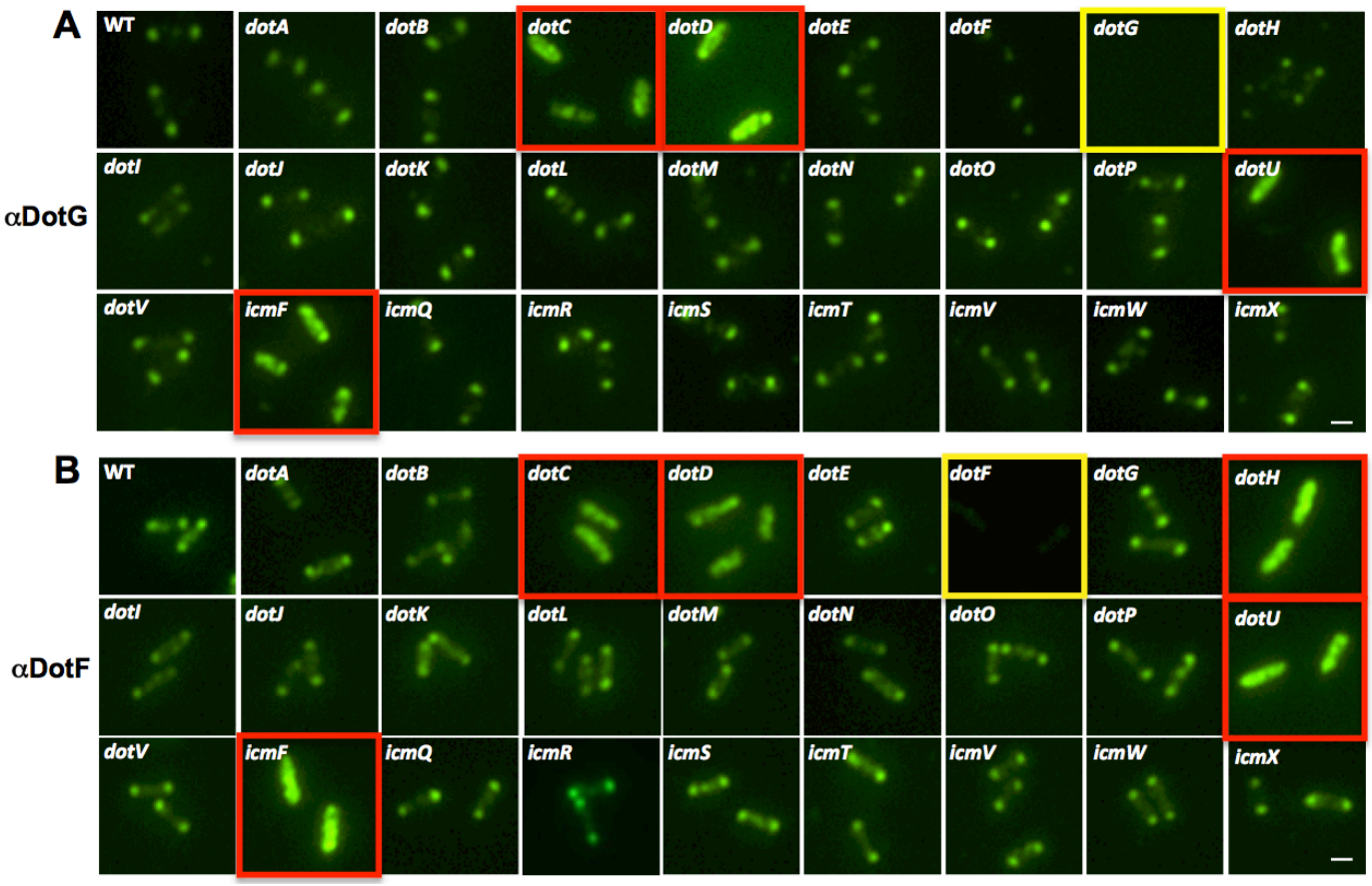

Supplementary Figure 16. (A,B) DotG and DotF localization in wild-type *Legionella* and in individual *dot/icm* deletions. DotG and DotF were detected by immunofluorescence microscopy in wild-type cells (WT) and individual *dot/icm* mutant strains. The corresponding deletion strains is boxed in yellow and *dot/icm* deletions that have an effect are boxed in red. Representative images are shown from three independent experiments. Scale bar: 2 μm (A,B).

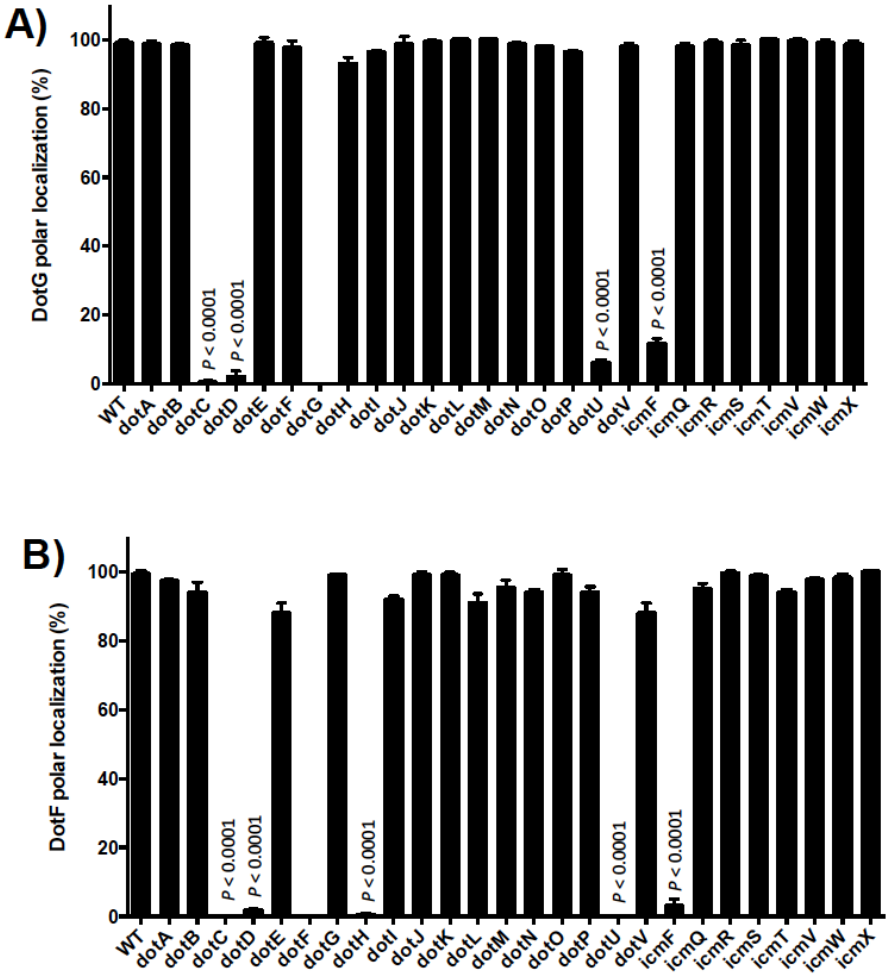

Supplementary Figure 17. (A,B) Quantitation of polar localization of DotG and DotF. The percent of cells having polar localization of the Dot proteins in individual *dot/icm* deletions was determined from three independent experiments (n=3) (100 cells counted from each experiment) and are shown in panels: DotG (A), and DotF (B). Data are presented as means ± SEM. P value indicates statistical difference compared to the wild-type strain Lp02 (WT) by unpaired two-tailed Student's t-test.

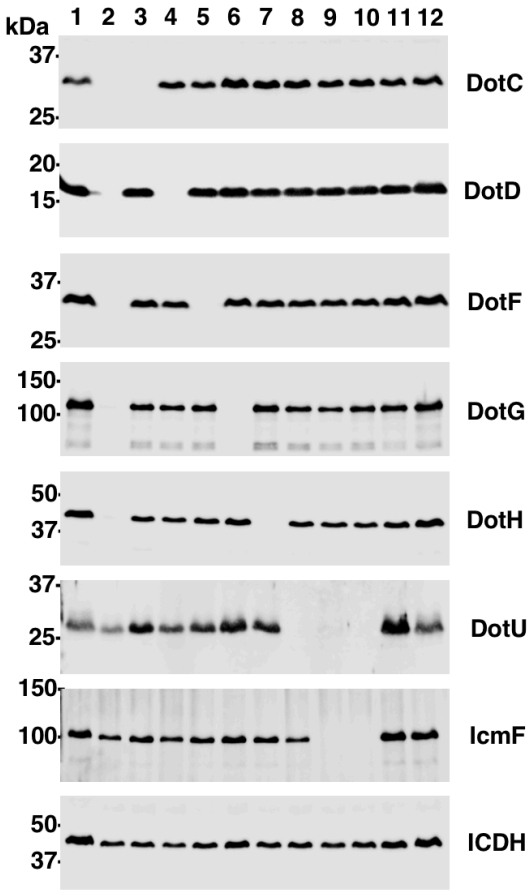

Supplementary Figure 18. Correct expression of DotC, DotD, DotF, DotG, DotH, DotU and IcmF in various strains in Figure 3B and Supplementary Figure 15. *L. pneumophila* strains were grown to late exponential phase and westerns were done with the indicated antibodies. ICDH, a cytoplasmic housekeeping protein, was used as a loading control. Samples were loaded in the following order: 1. JV1139 (Lp02 + pJB908), 2. JV5402 (SΔ(UF) + vector), 3. JV3743 (Δ*dotC*), 4. JV3572 (Δ*dotD*), 5. JV3579 (Δ*dotF*), 6. JV3559 (Δ*dotG*), 7. JV3563 (Δ*dotH*), 8. JV4015 (Δ*dotU*), 9. JV1179 (Δ*icmF*), 10. JV1196 (Δ*dotU* Δ*icmF* + vector), 11. JV1199 (Δ*dotU* Δ*icmF* + *dotU icmF*), 12. JV1139 (Lp02 + pJB908). Each of these experiments were done three times and representative blots are shown.

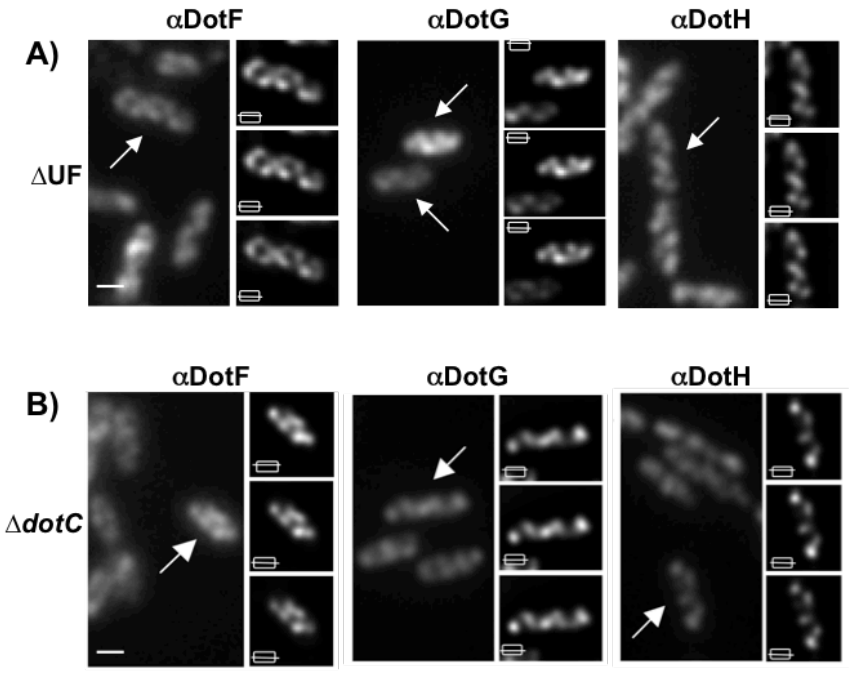

Supplementary Figure 19. DotF, DotG and DotH proteins are found in non-polar punctae in the Δ*dotU* Δ*icmF* (ΔUF) and the Δ*dotC* mutants. DotF, DotG, and DotH localization was assayed using a lower amount of primary antibody and deconvolution microscopy. For each strain, four images are shown including an optical section before deconvolution (left) and three images of a top optical section, a middle optical section, and a bottom optical section (right panel). Arrows in the left image indicate the cell that was deconvoluted. Representative images from three independent experiments are shown for the ΔUF mutant (A) and the Δ*dotC* mutant (B). Scale bar 2 μm.

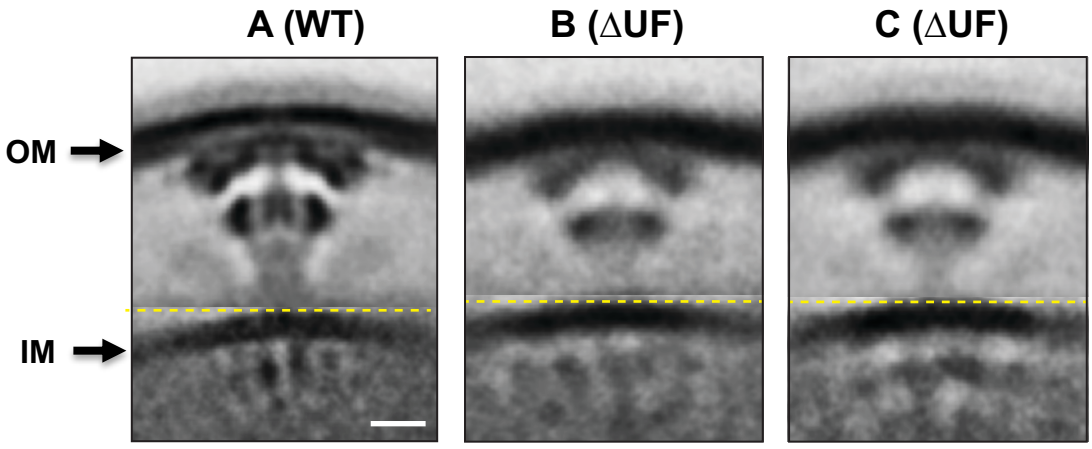

Supplementary Figure 20. Comparison of T4SS complexes in the wild-type (WT) strain and the Δ*dotU* Δ*icmF* (ΔUF) mutant by ECT analysis.Shown are central slices through the sub-tomogram averages of polar WT complexes (A), non-polar ΔUF complexes (B) and polar ΔUF complexes (C). Approximately the same numbers of polar and non-polar complexes were detected in the ΔUF mutant (240 polar and 202 non-polar particles). However, only about one quarter as many complexes were detected in the ΔUF mutant compared to a wild-type cell (1.8 complexes versus 7.6 complexes, respectively) likely due to the failure to assemble a visible DotHCD subcomplex in the absence of UF. In addition, the complexes that were observed resolved poorly due to decreased stability of the T4BSS apparatus. In WT cells, no non-polar complexes were detected in ~2000 cells. Scale bar 10 nm (A-C). Number of tomograms and particles used for the subtomogram average are listed in Supplementary Information Table 1.

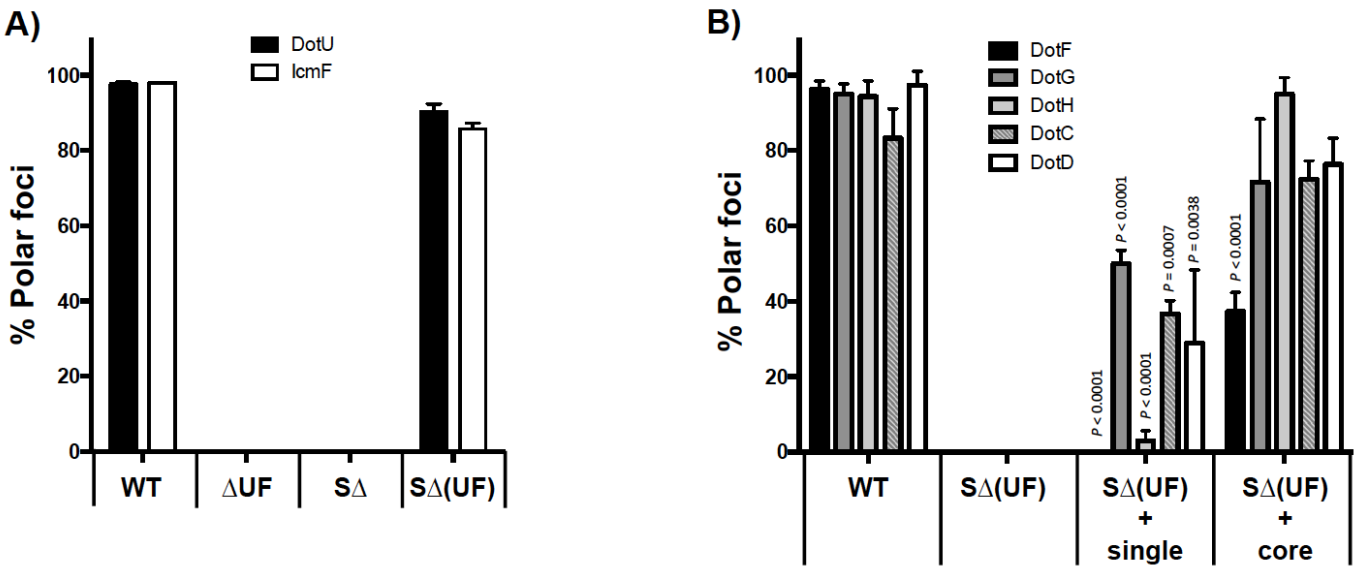

Supplementary Figure 21. Quantitation of polar localization of Dot proteins for Figure 4. The percent of cells having polar localization of the DotU and IcmF proteins (A) and DotF, DotG, DotH, DotC, and DotD (B) in the wild-type strain Lp02 (WT), Δ*dotU* Δ*icmF* mutant strain (JV1181), the super *dot/icm* deletion strain (SΔ, JV4044) and the SΔ strain expressing *dotU* and *icmF* from the chromosome (SΔ(UF)), JV5319) was determined from three independent experiments (n=3) (100 cells counted from each experiment). Data are presented as means ± SEM. P valueindicates statistical difference compared to the wild-type strain Lp02 (WT) by unpaired two-tailed Student's t-test.

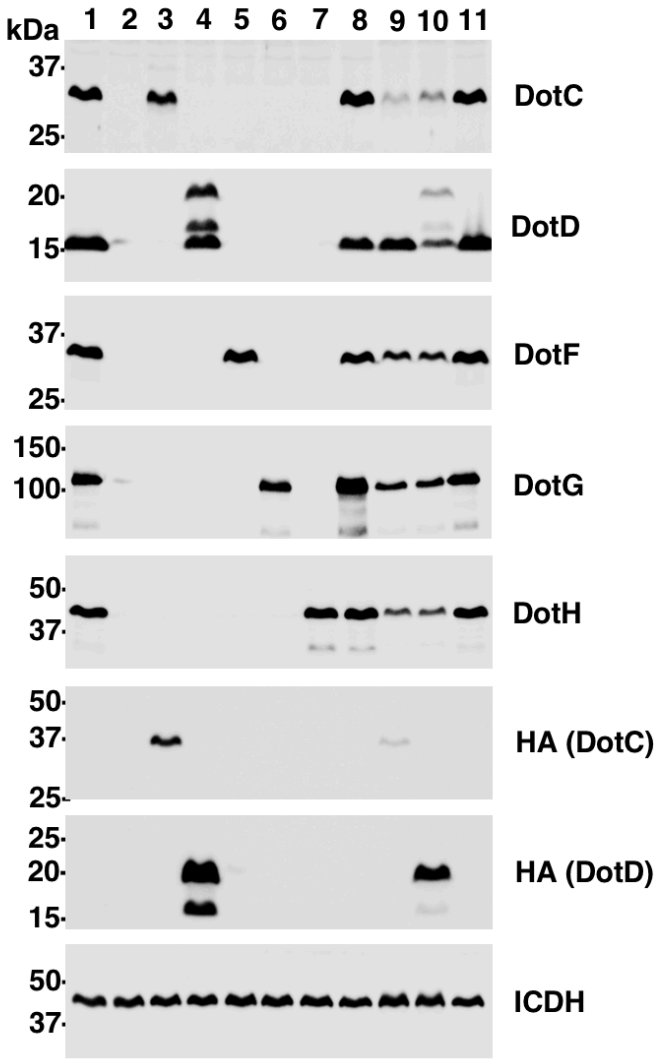

Supplementary Figure 22. Expression of the correct components in the SΔ(UF) strain for Figure 4. *L. pneumophila* strains were grown to late exponential phase and westerns were done with the indicated antibodies. ICDH, a cytoplasmic housekeeping protein, was used as a loading control. Samples were loaded in the following order: 1. JV1139 (Lp02 + pJB908), 2. JV5402 (SΔ(UF) + vector), 3. JV5410 (SΔ(UF) + *dotC:HA3X*), 4. JV5411 (SΔ(UF) + *dotD:HA3X*), 5. JV5403 (SΔ(UF) + *dotF*), 6. JV5404 (SΔ(UF) + *dotG*), 7. JV5405 (SΔ(UF) + *dotH*), 8. JV5443 (SΔ(UF) + *dotCDFGH*), 9. JV5750 (SΔ(UF) + *dotC:HA3x dotD dotH*), 10. JV5751 (SΔ(UF) + *dotD:HA3x dotC dotH*), 11. JV1139 (Lp02 + pJB908). Each of these experiments were done three times and representative blots are shown.

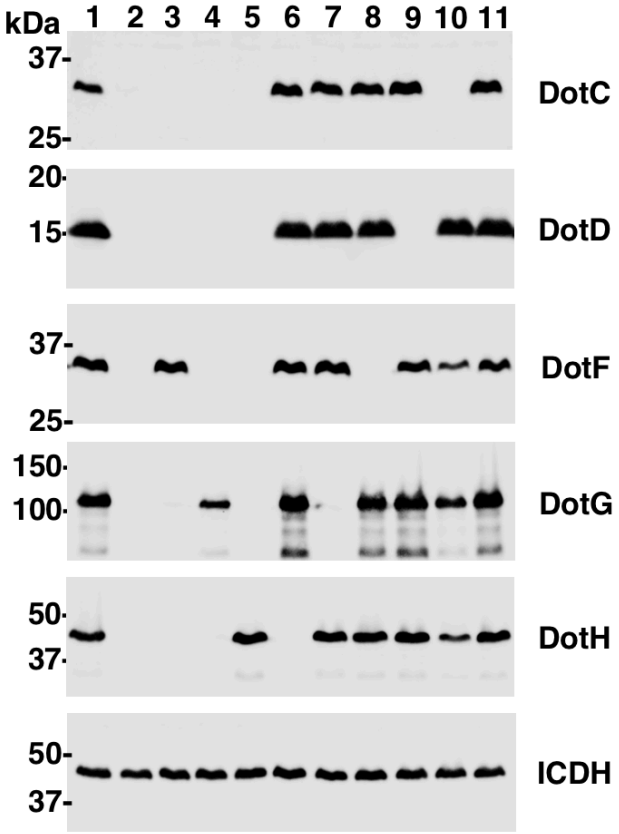

Supplementary Figure 23. Expression of the correct single and quadruple combinations in the reconstituted SΔ(UF) strain for Figure 5 and Supplementary Figure 28. *L. pneumophila* strains were grown to late exponential phase and westerns were done with the indicated antibodies. ICDH, a cytoplasmic housekeeping protein, was used as a loading control. Samples were loaded in the following order: 1. JV1139 (Lp02 + pJB908), 2. JV5402 (SΔ(UF) + vector), 3. JV5403 (SΔ(UF) + *dotF*), 4. JV5404 (SΔ(UF) + *dotG*), 5. JV5405 (SΔ(UF) + *dotH*), 6. JV5468 (SΔ(UF) + *dotCDFG*), 7. JV5466 (SΔ(UF) + *dotCDFH*), 8. JV5475 (SΔ(UF) + *dotCDGH*), 9. JV5439 (SΔ(UF) + *dotCFGH*), 10. JV5441 (SΔ(UF) + *dotDFGH*), 11. JV5443 (SΔ(UF) + *dotCDFGH*). Each of these experiments were done three times and representative blots are shown.

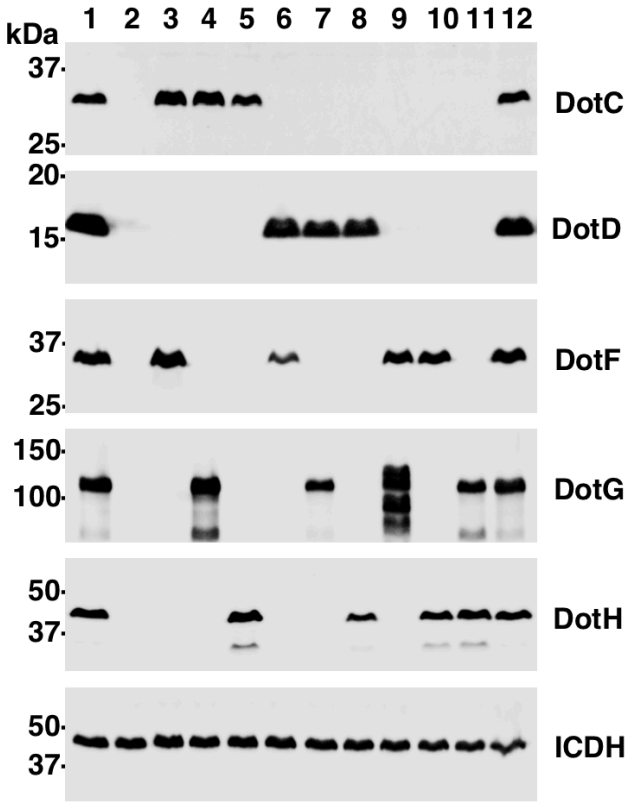

Supplementary Figure 24. Expression of the correct double combinations in the reconstituted SΔ(UF) strain for Figure 5 and Supplementary Figure 28. *L. pneumophila* strains were grown to late exponential phase and westerns were done with the indicated antibodies. ICDH, a cytoplasmic housekeeping protein, was used as a loading control. Samples were loaded in the following order: 1. JV1139 (Lp02 + pJB908), 2. JV5402 (SΔ(UF) + vector), 3. JV5452 (SΔ(UF) + *dotCF*), 4. JV5455 (SΔ(UF) + *dotCG*), 5. JV5458 (SΔ(UF) + *dotCH*), 6. JV5453 (SΔ(UF) + *dotDF*), 7. JV5456 (SΔ(UF) + *dotDG*), 8. JV5459 (SΔ(UF) + *dotDH*), 9. JV5408 (SΔ(UF) + *dotFG*), 10. JV5407 (SΔ(UF) + *dotFH*), 11. JV5406 (SΔ(UF) + *dotGH*), 12. JV1139 (Lp02 + pJB908). Each of these experiments were done three times and representative blots are shown.

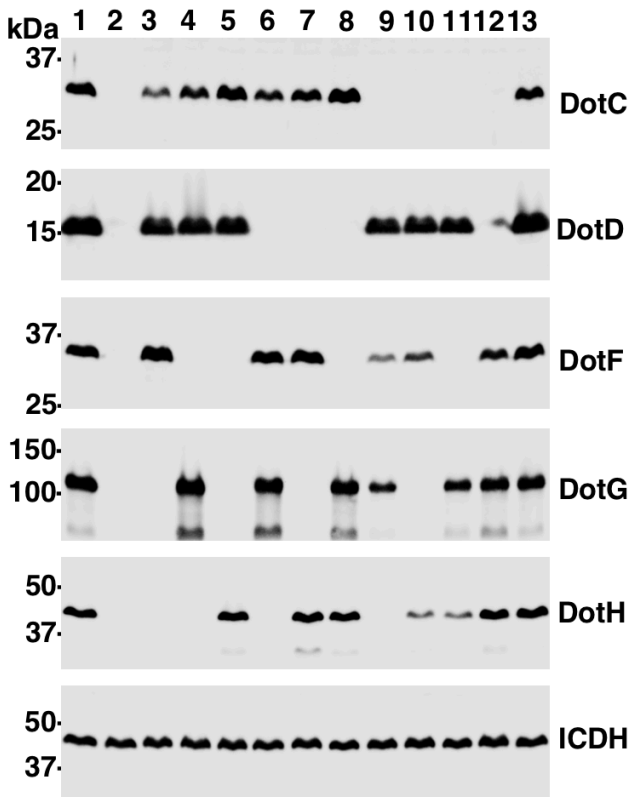

Supplementary Figure 25. Expression of the correct triple combinations in the reconstituted SΔ(UF) strain for Figure 5 and Supplementary Figure 28. *L. pneumophila* strains were grown to late exponential phase and westerns were done with the indicated antibodies. ICDH, a cytoplasmic housekeeping protein, was used as a loading control. Samples were loaded in the following order: 1. JV1139 (Lp02 + pJB908), 2. JV5402 (SΔ(UF) + vector), 3. JV5454 (SΔ(UF) + *dotCDF*), 4. JV5457 (SΔ(UF) + *dotCDG*), 5. JV5460 (SΔ(UF) + *dotCDH*), 6. JV5467 (SΔ(UF) + *dotCFG*), 7. JV5464 (SΔ(UF) + *dotCFH*), 8. JV5473 (SΔ(UF) + *dotCGH*), 9. JV5472 (SΔ(UF) + *dotDFG*), 10. JV5465 (SΔ(UF) + *dotDFH*), 11. JV5474 (SΔ(UF) + *dotDGH*), 12. JV5409 (SΔ(UF) + *dotFGH*), 13. JV1139 (Lp02 + pJB908). Each of these experiments were done three times and representative blots are shown.

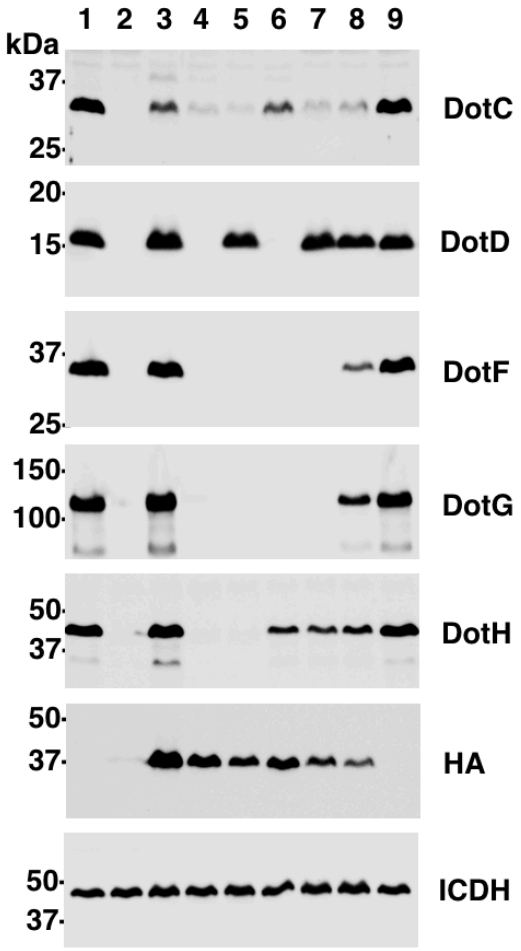

Supplementary Figure 26. Expression of the correct components in the reconstituted SΔ(UF) strain containing HA-tagged proteins Figure 5 and Supplementary Figure 28. *L. pneumophila* strains were grown to late exponential phase and westerns were done with the indicated antibodies. ICDH, a cytoplasmic housekeeping protein, was used as a loading control. Samples were loaded in the following order: 1. JV1139 (Lp02 + pJB908), 2. JV5402 (SΔ(UF) + vector), 3. JV5484 (Δ*dotC* + *dotC:HA3x*), 4. JV5480 (SΔ(UF) + *dotC:HA3x*), 5. JV5482 (SΔ(UF) + *dotC:HA3x dotD*), 6. JV5749 (SΔ(UF) + *dotC:HA3x dotH*), 7. JV5750 (SΔ(UF) + *dotC:HA3x dotD dotH*), 8. JV5752 (SΔ(UF) + *dotC:HA3x dotD dotFGH*), 9. JV1139 (Lp02 + pJB908). Each of these experiments were done three times and representative blots are shown.

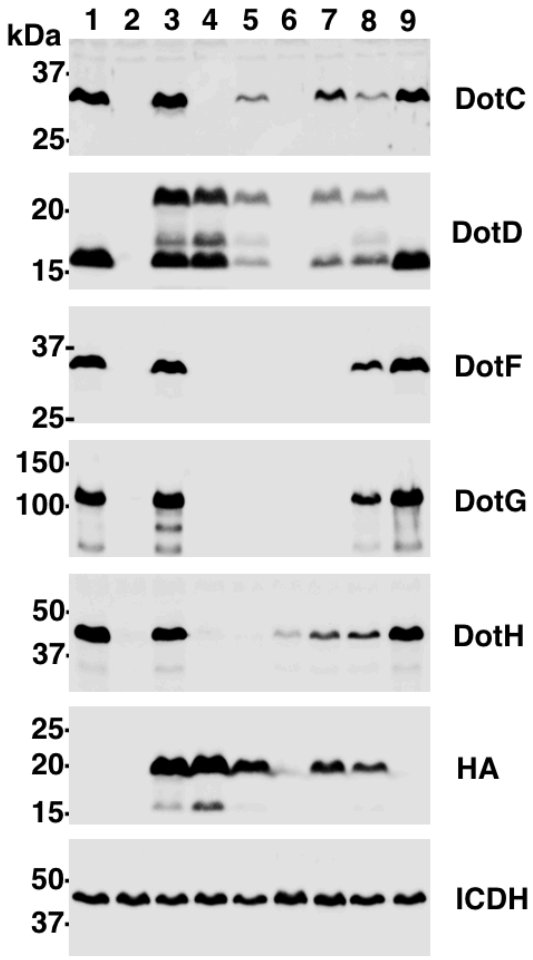

Supplementary Figure 27. Expression of the correct components in the reconstituted SΔ(UF) strain containing HA-tagged proteins for Figure 5 and Supplementary Figure 28. *L. pneumophila* strains were grown to late exponential phase and westerns were done with the indicated antibodies. ICDH, a cytoplasmic housekeeping protein, was used as a loading control. Samples were loaded in the following order: 1. JV1139 (Lp02 + pJB908), 2. JV5402 (SΔ(UF) + vector), 3. JV5484 (Δ*dotD* + *dotD:HA3x*), 4. JV5480 (SΔ(UF) + *dotD:HA3x*), 5. JV5482 (SΔ(UF) + *dotD:HA3x dotC*), 6. JV5749 (SΔ(UF) + *dotD:HA3x dotH*), 7. JV5750 (SΔ(UF) + *dotD:HA3x dotC dotH*), 8. JV5752 (SΔ(UF) + *dotD:HA3x dotC dotFGH*), 9. JV1139 (Lp02 + pJB908). Each of these experiments were done three times and representative blots are shown.

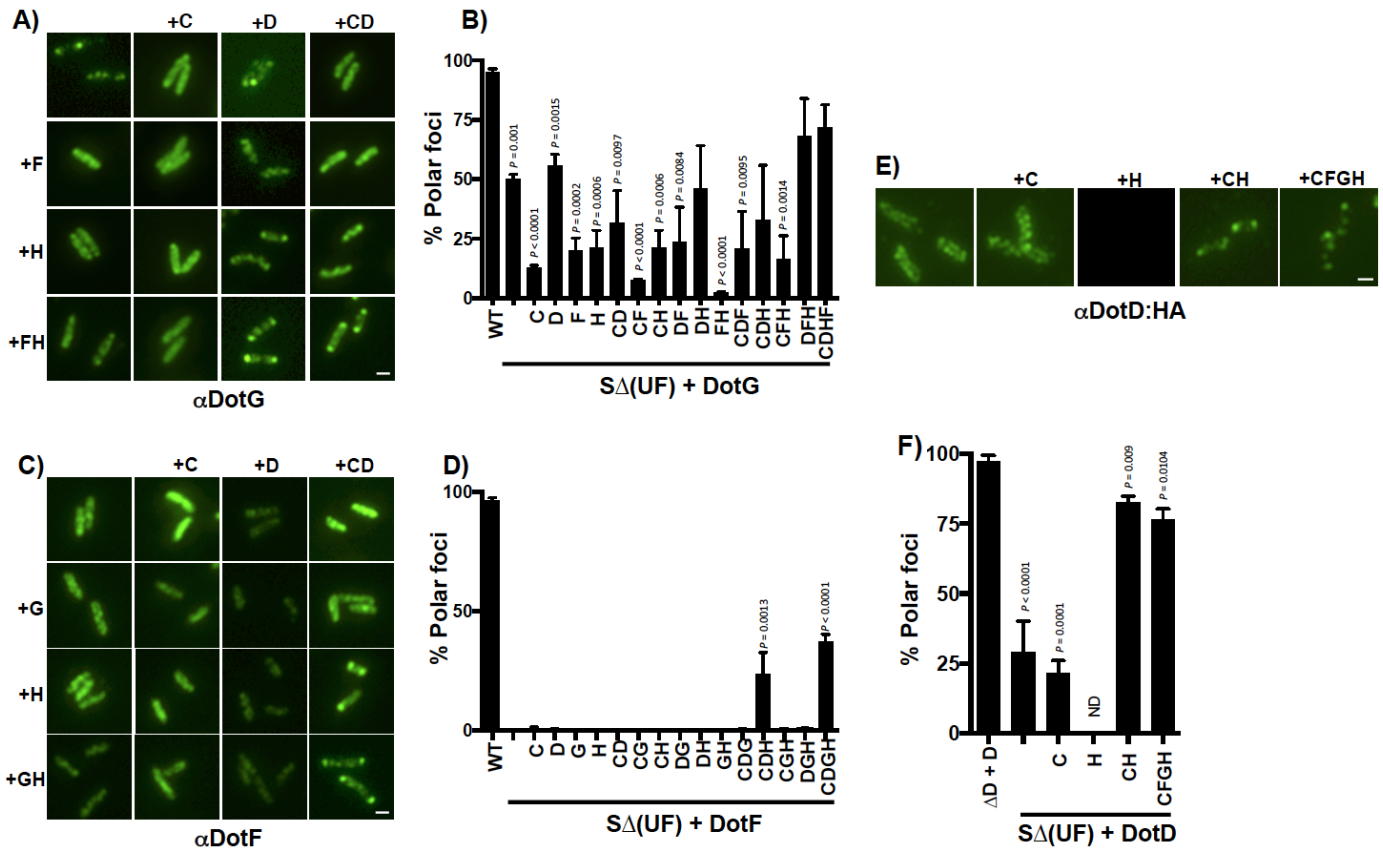

Supplementary Figure 28. Reconstitution of the core-transmembrane subcomplex in the SΔ(UF) strain. Combinations of the five components of the core-transmembrane subcomplex were expressed in the super *dot/icm* deletion strain encoding *dotU* and *icmF* (SΔ(UF)). Representative images for DotG, DotF, and DotD-HA localization are shown (A, C, E, respectively). Proteins expressed in each strain is indicated by labels on the left and top of each panel and the protein localized by IFM is shown below the images. The percent of cells having polar localization of the Dot proteins was determined from three independent experiments (n=3) (100 cells counted from each experiment) and are shown in panels B, D, and F. Data are presented as means ± SEM. P value indicates statistical difference compared to the wild-type strain Lp02 (WT) by unpaired two-tailed Student's t-test. Scale bar: 2 μm.

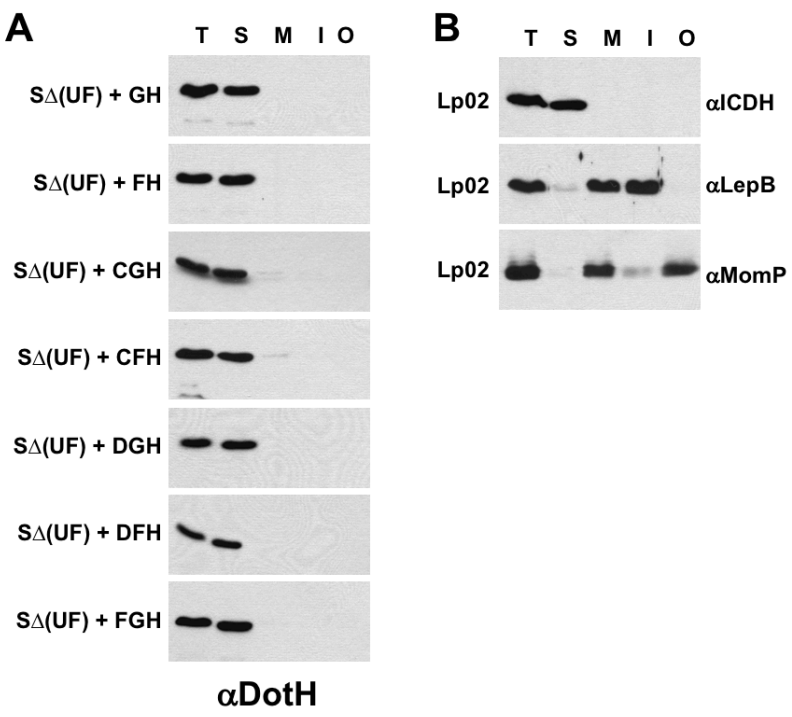

Supplementary Figure 29. DotH localization to the outer membrane requires the anchor proteins DotU and IcmF. Cells were fractionated by a combination of ultracentrifugation and Triton X-100 solubility, proteins were separated by SDS-PAGE and probed in westerns using DotH specific antibodies. (A) SΔ(UF) strains that did not restore DotH outer membrane localization include: DotG/DotH (JV5406), DotF/DotH (JV5407), DotC/DotG/DotH (JV5460), DotC/DotF/DotH (JV5464), DotG/DotF/DotH (JV5409), DotD/DotF/DotH (JV5465) and DotF/DotG/DotH (JV5409). (B) Controls for the fractionations are shown and include the cytoplasmic protein isocitrate dehydrogenase (ICDH), the inner membrane protein LepB and the outer membrane protein MomP. Experiments were done in triplicate and representative images are shown. Each of these experiments were done three times and representative blots are shown.

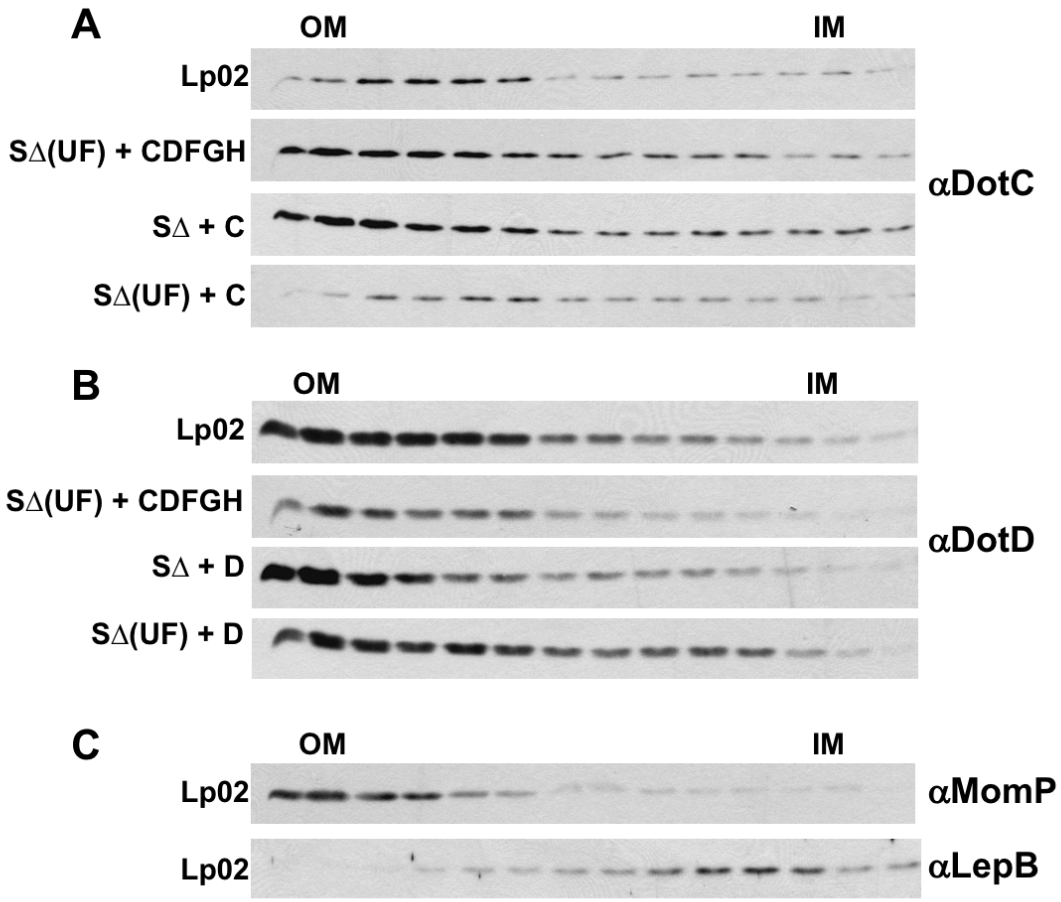

Supplementary Figure 30. Lipoproteins DotC and DotD remain in the outer membrane in the presence and absence of DotU and IcmF. Strains were grown to late exponential phase, total membrane was isolated and separated by sucrose density gradient. Fractions were then separated by SDS-PAGE and probed using DotC or DotD specific antibodies (indicated to the right of the blots). (A) Wild-type *Legionella* Lp02, SΔ(UF) + core (JV5443), SΔ + DotC (JV4225), and SΔ(UF) + DotC (JV5410). (B) Wild-type *Legionella* Lp02, SΔ(UF) + core (JV5443), SΔ + DotD (JV4695), and SΔ(UF) + DotD (JV5411). (C) Controls include the outer membrane protein MomP and the inner membrane protein LepB. Each of these experiments were done three times and representative blots are shown.

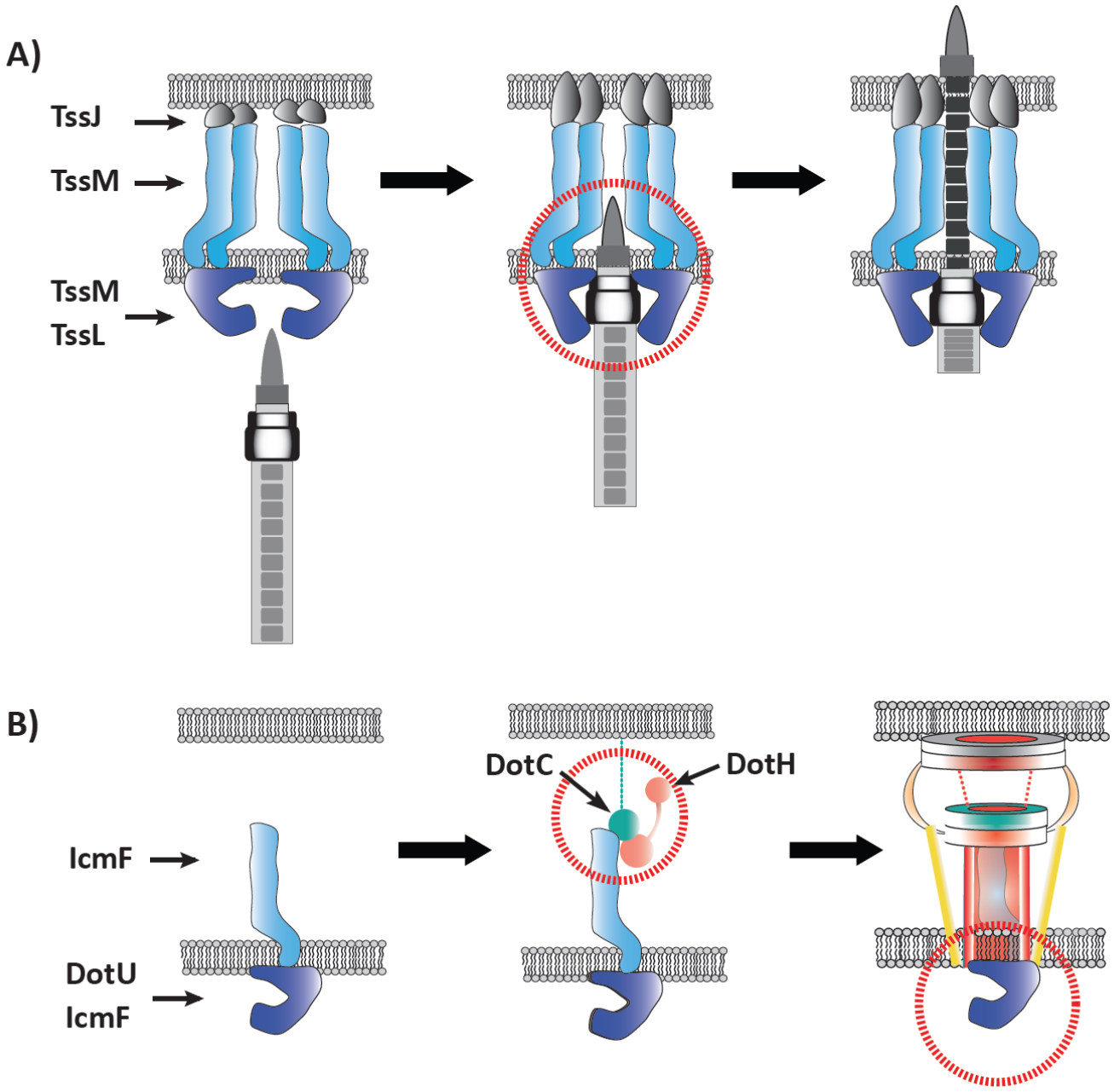

Supplementary Figure 31. A-B Polar targeting and assembly of the *Legionella* core-transmembrane subcomplex by DotU and IcmF. (A) The T6SS core membrane complex is made up of TssJ, TssL, and TssM and is used as a docking station for the baseplate and tail (red circle). (B) DotU and IcmF resemble components of the T6SS core membrane complex but lack a homolog to the lipoprotein TssJ. Instead DotU and IcmF recruit the lipoprotein DotC and DotH (red circle in the center panel). Upon assembly of the *Legionella* core transmembrane complex, it is possible that the cytoplasmic domains of DotU and IcmF recruit additional components of the Dot/Icm apparatus (red circle in the right panel).

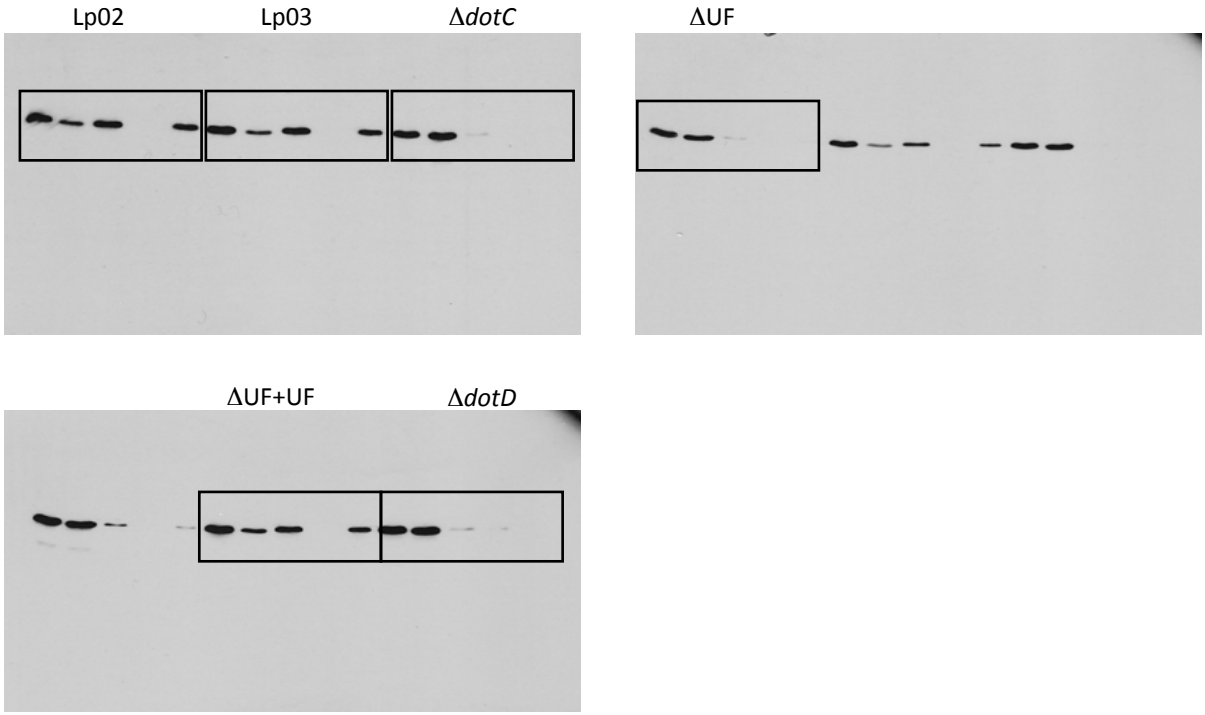

Supplementary Figure 32A. Full length western blots used to generate Fig. 5E (αDotH). Boxes represent the sections that were used.

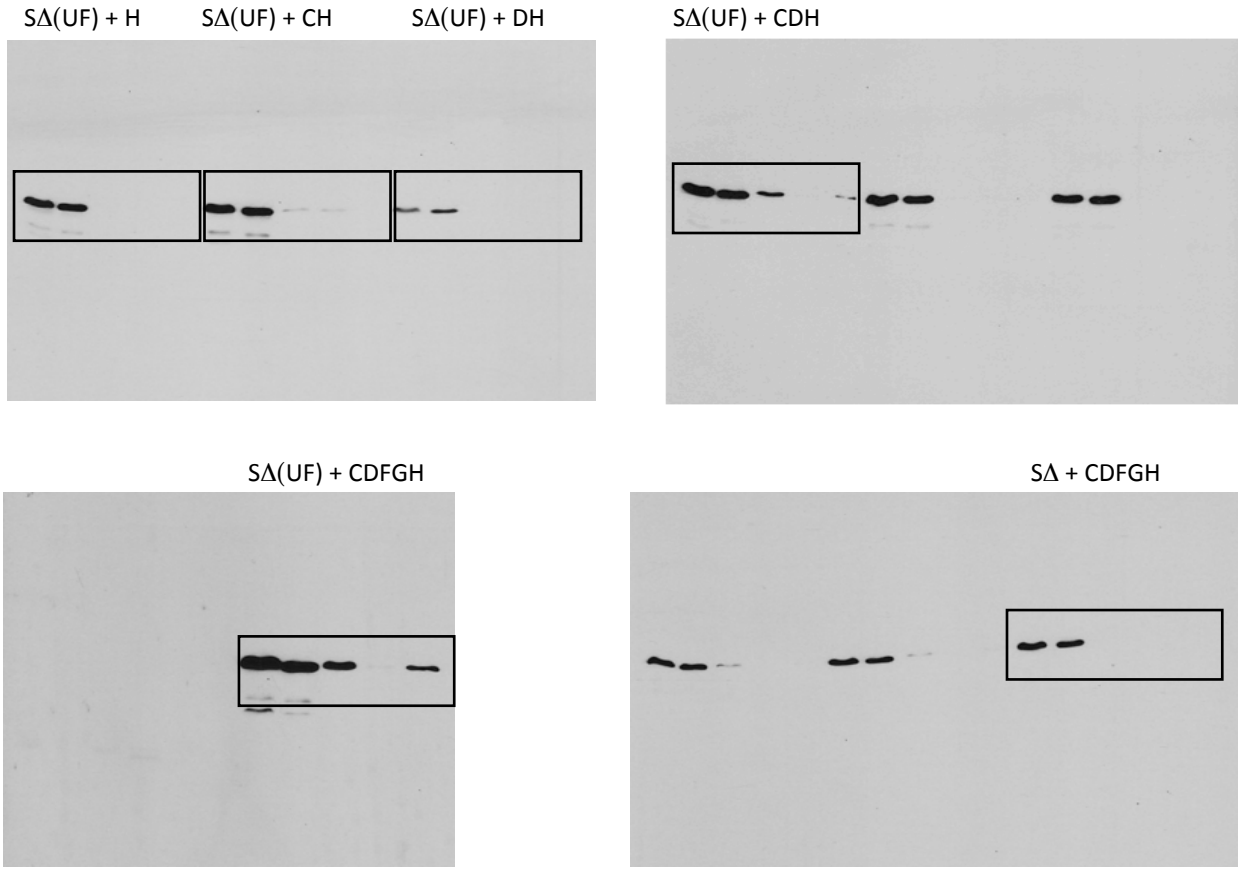

Supplementary Figure 32B. Full length western blots used to generate Fig. 5F (αDotH). Boxes represent the sections that were used.

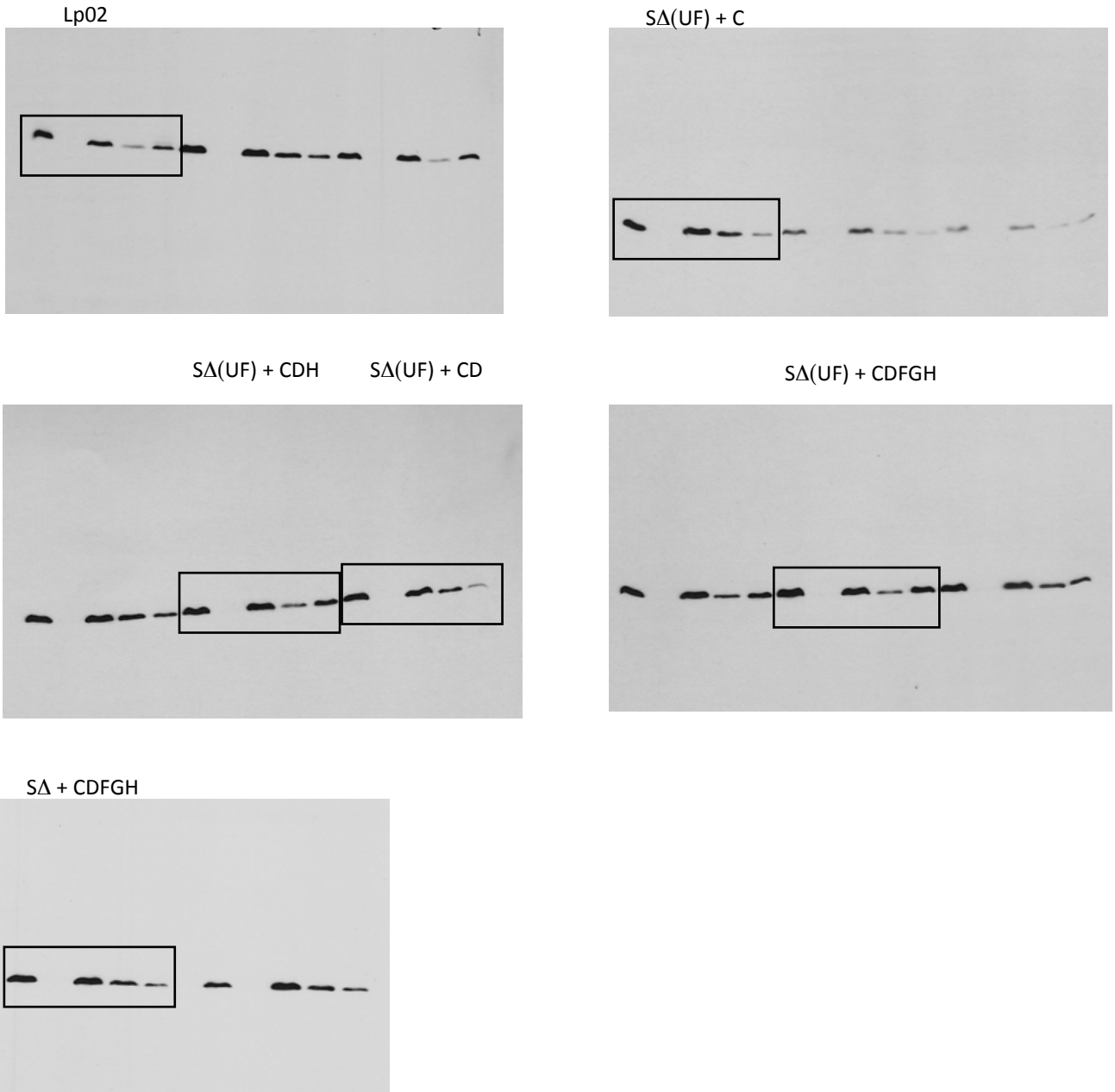

Supplementary Figure 32C. Full length western blots used to generate Fig. 5G (αDotC). Boxes represent the sections that were used.

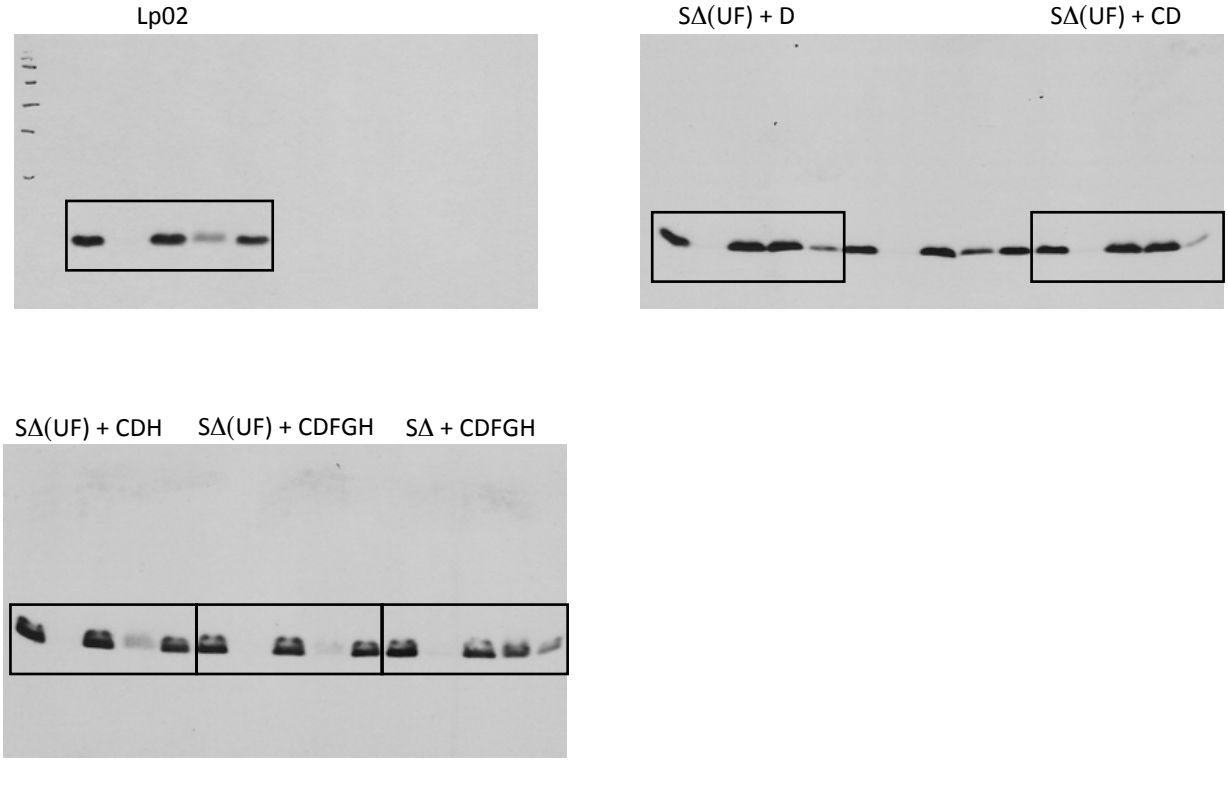

Supplementary Figure 32D. Full length western blots used to generate Fig. 5H (αDotD). Boxes represent the sections that were used.

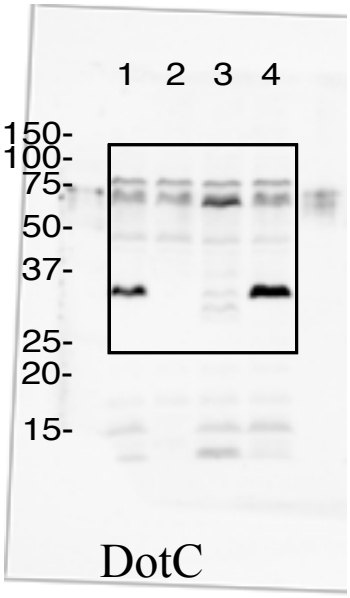

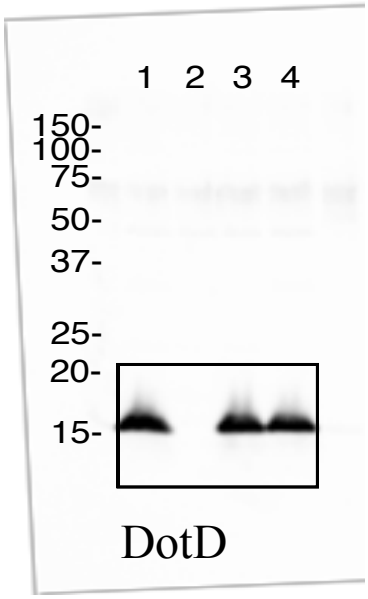

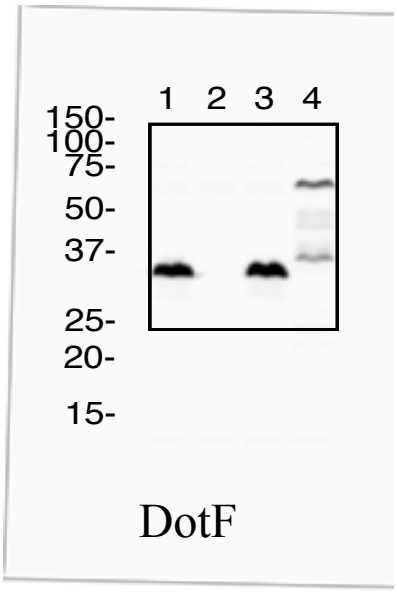

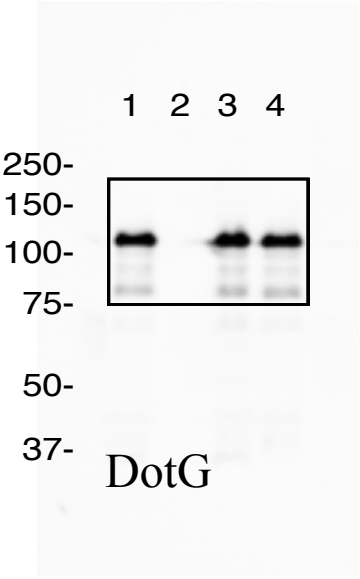

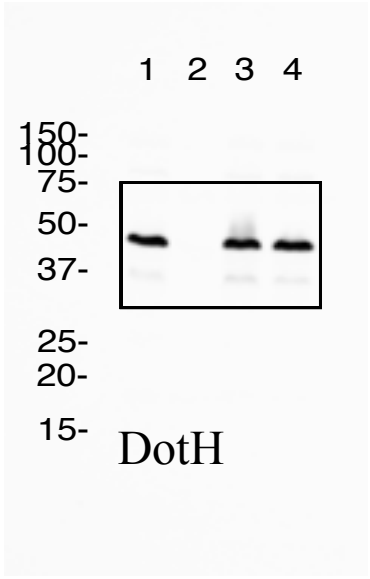

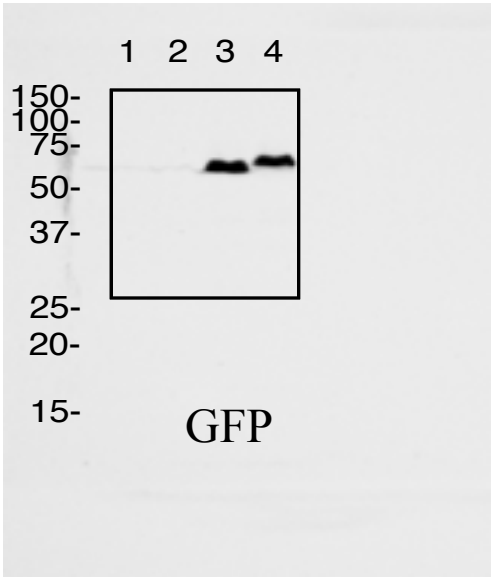

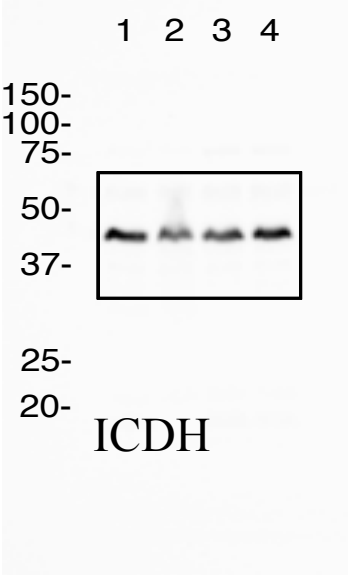

Supplementary Figure 32E. Full length western blots used to generate Supplementary Figure 2a. Boxes represent the sections that were used.

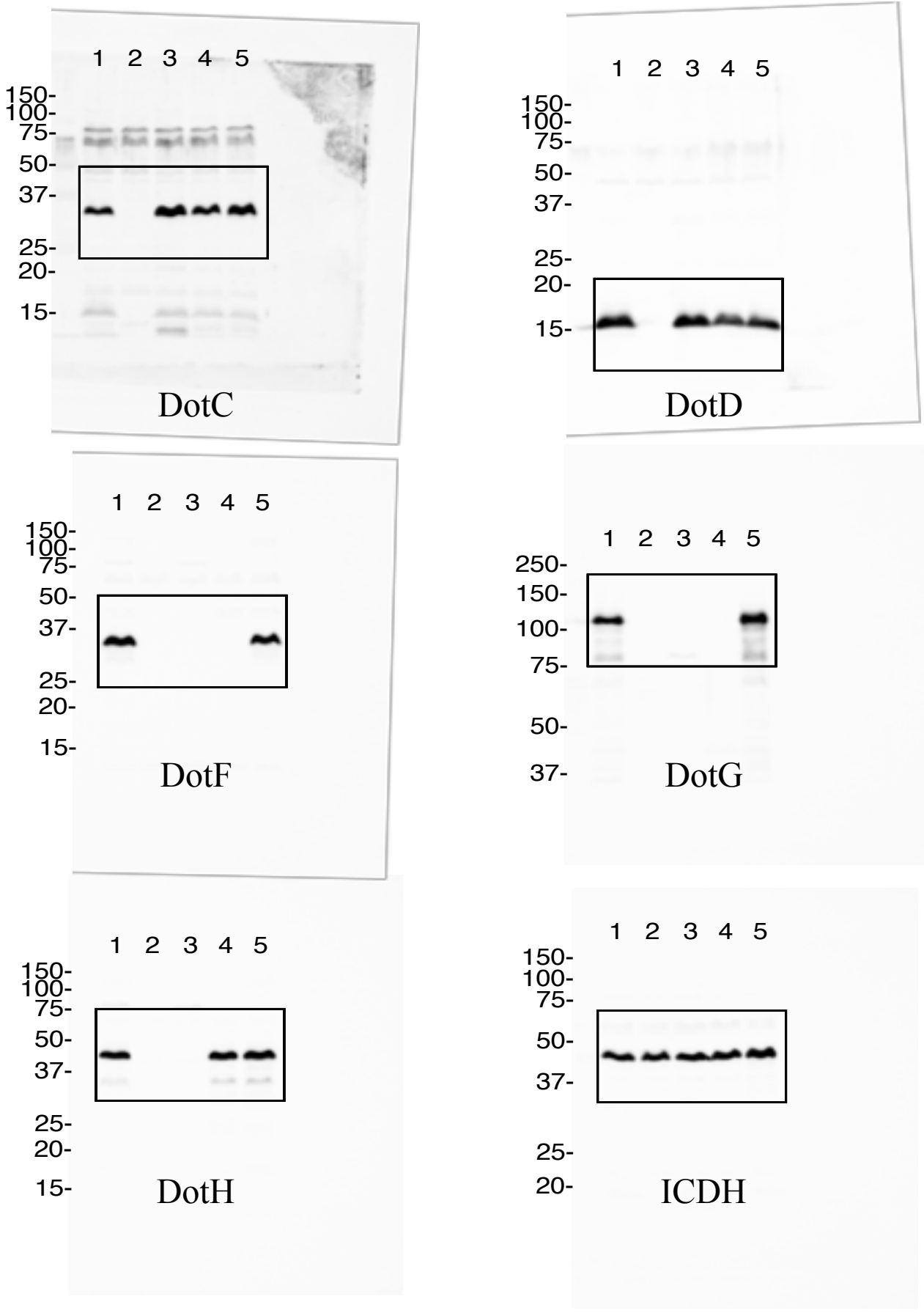

Supplementary Figure 32F. Full length western blots used to generate Supplementary Figure 2b. Boxes represent the sections that were used.

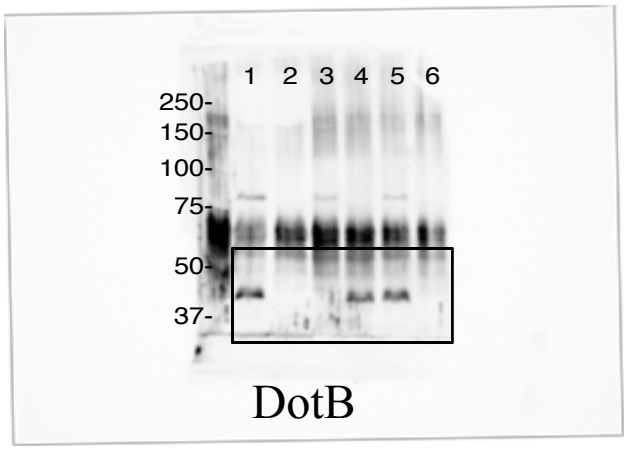

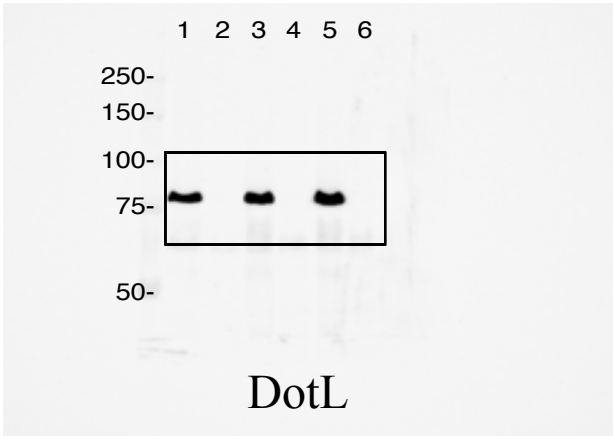

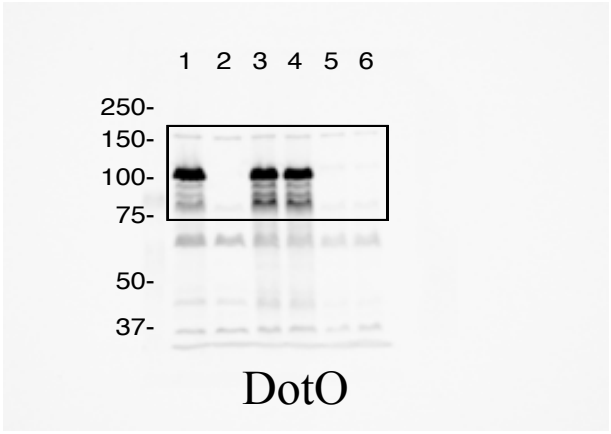

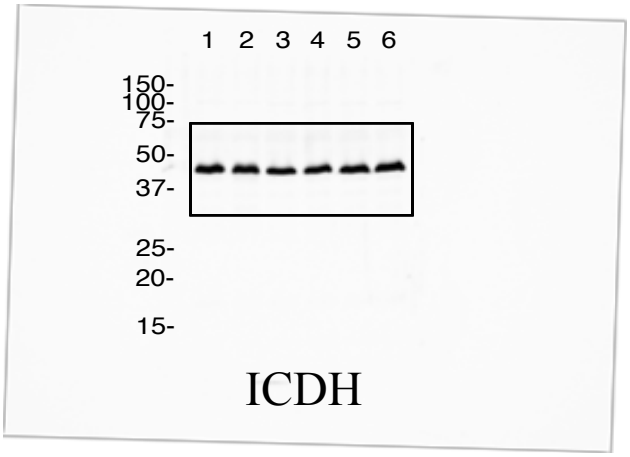

Supplementary Figure 32G. Full length western blots used to generate Supplementary Figure 2c. Boxes represent the sections that were used.

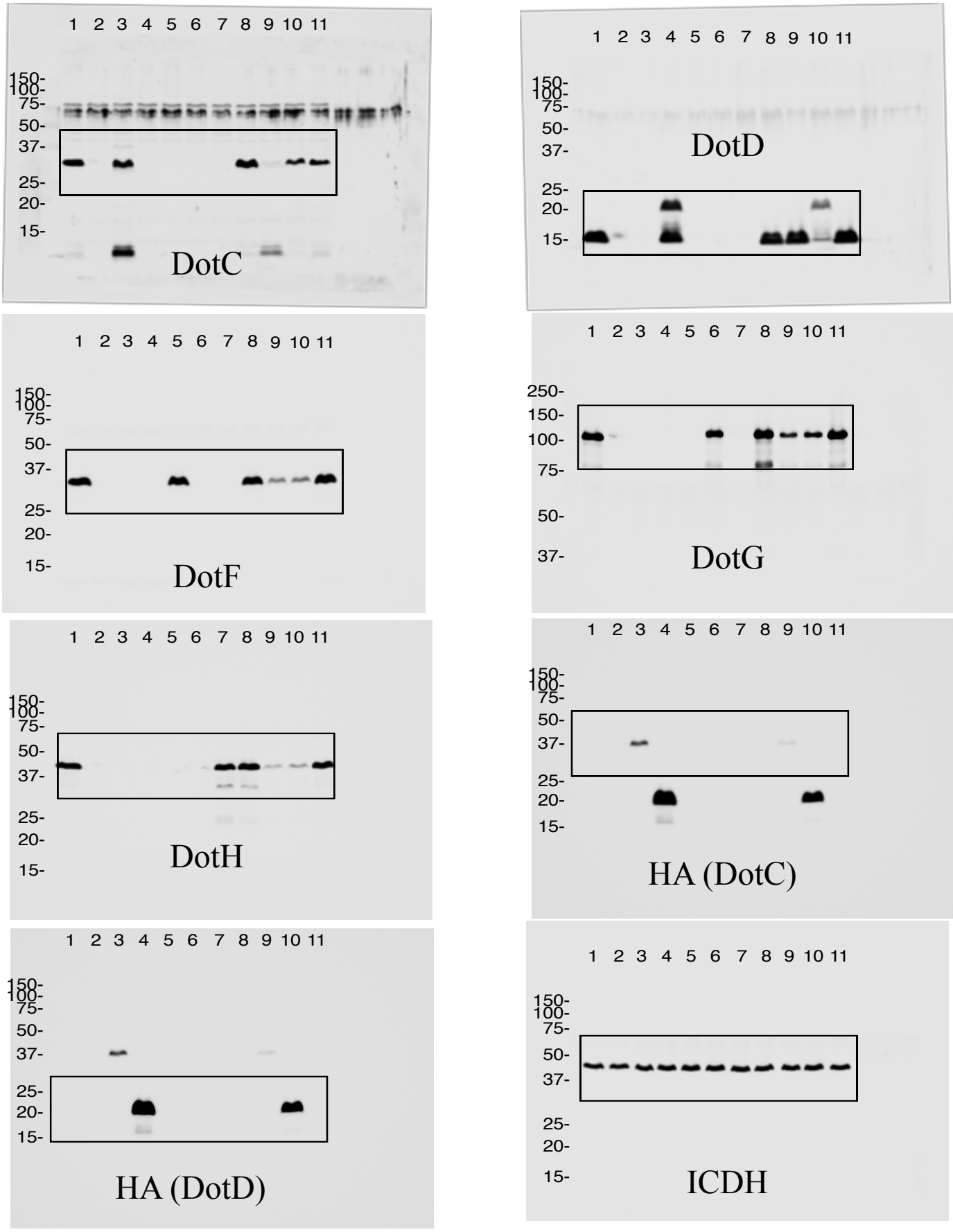

Supplementary Figure 32H. Full length western blots used to generate Supplementary Figure 14. Boxes represent the sections that were used.

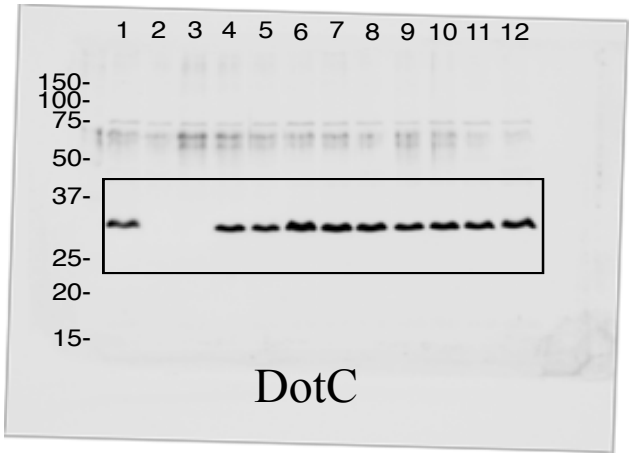

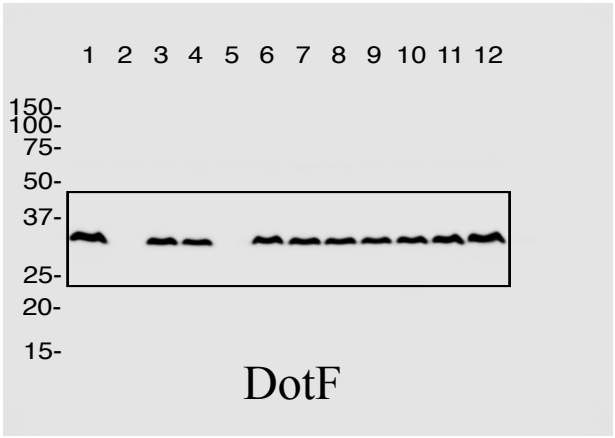

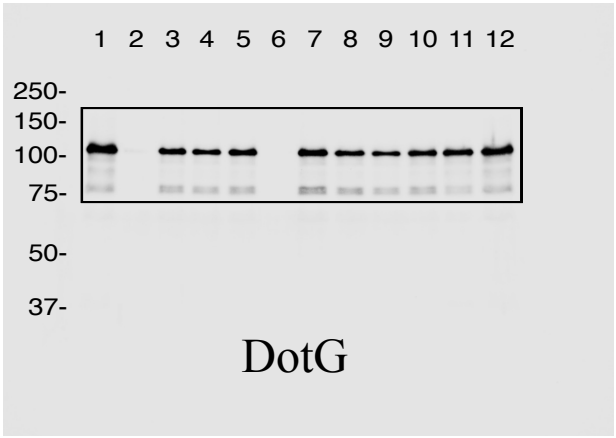

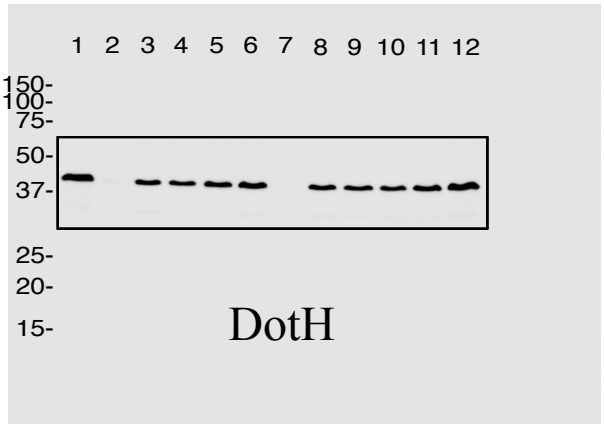

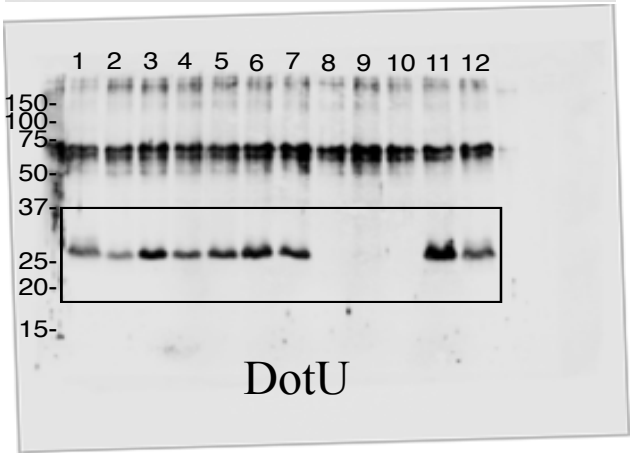

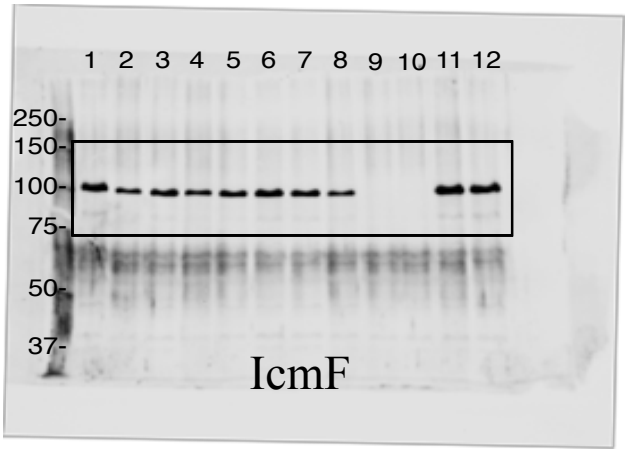

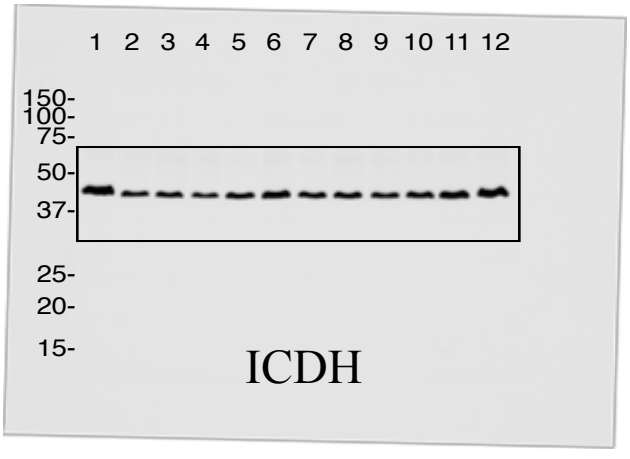

Supplementary Figure 32I. Full length western blots used to generate Supplementary Figure 18. Boxes represent the sections that were used.

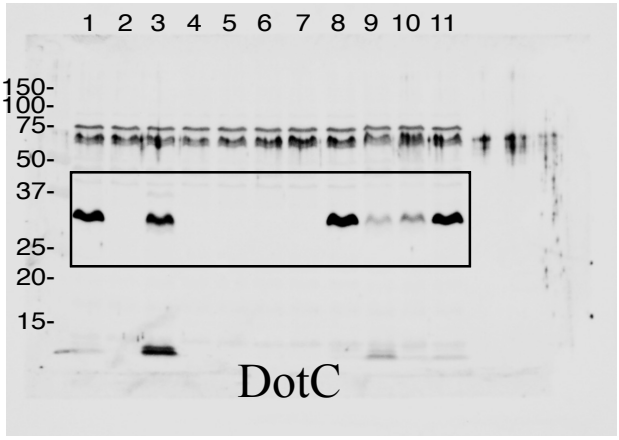

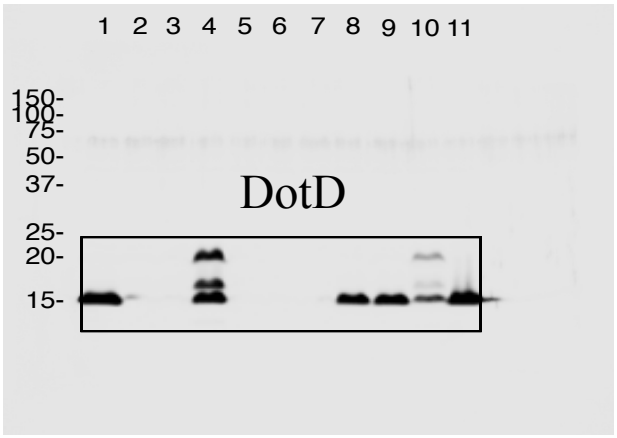

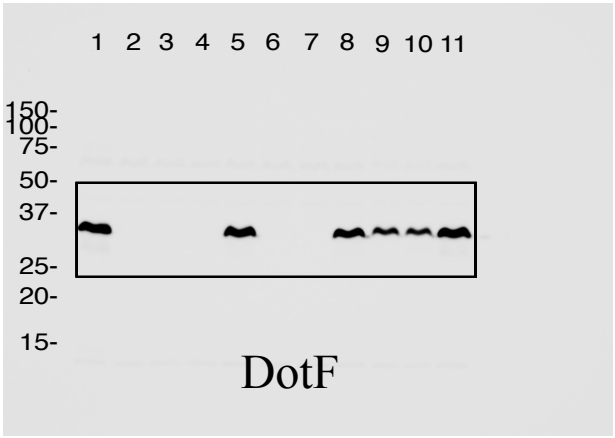

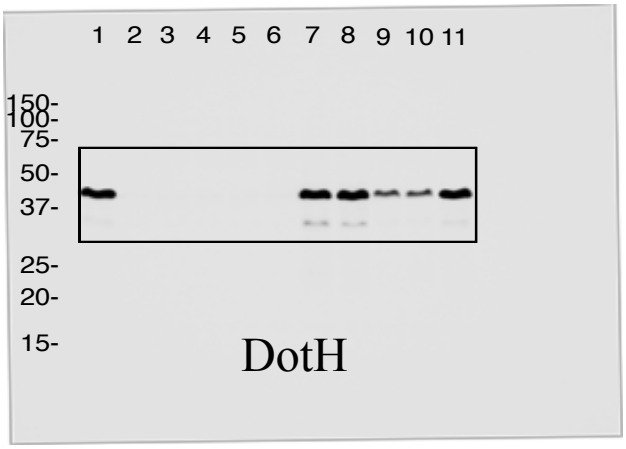

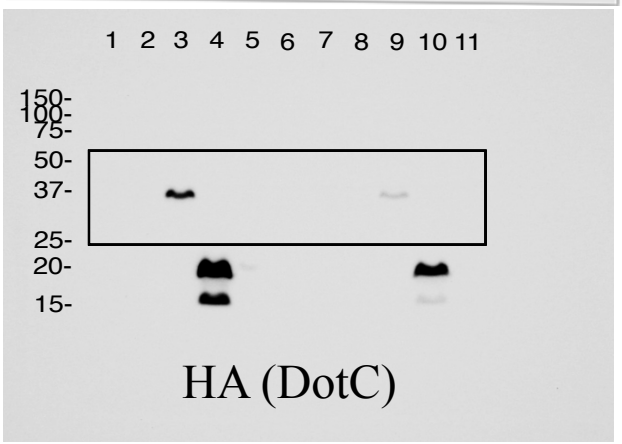

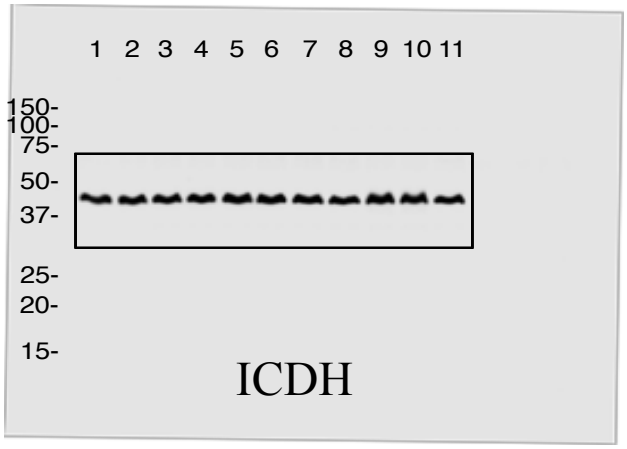

Supplementary Figure 32J. Full length western blots used to generate Supplementary Figure 22. Boxes represent the sections that were used.

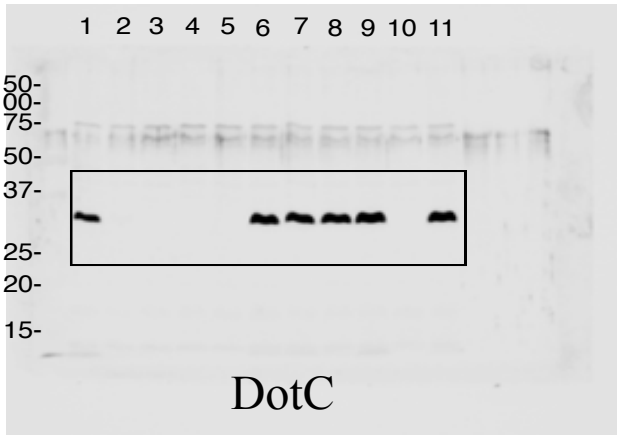

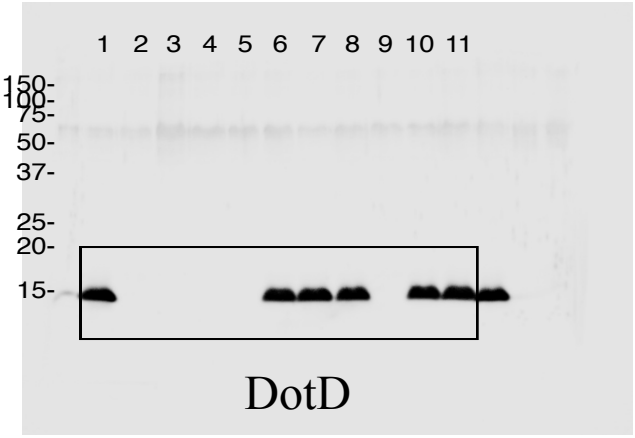

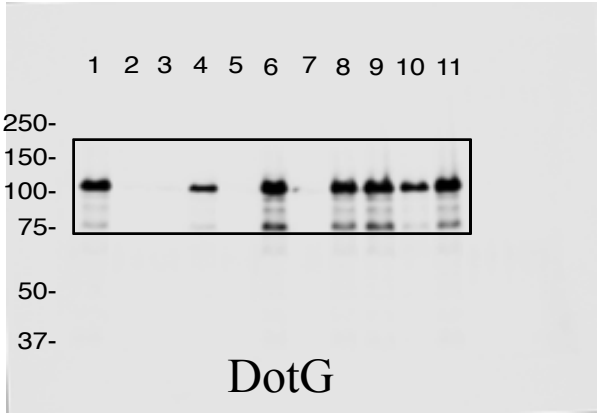

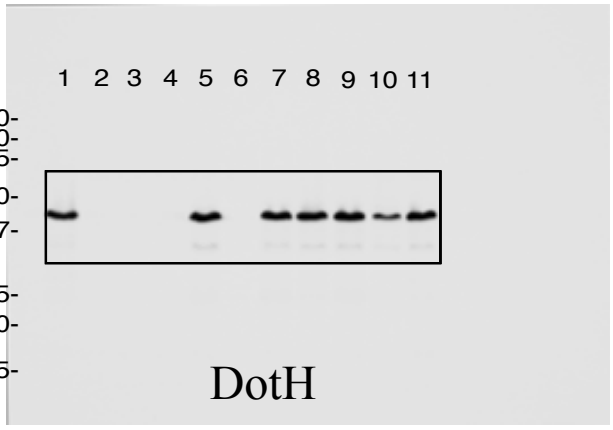

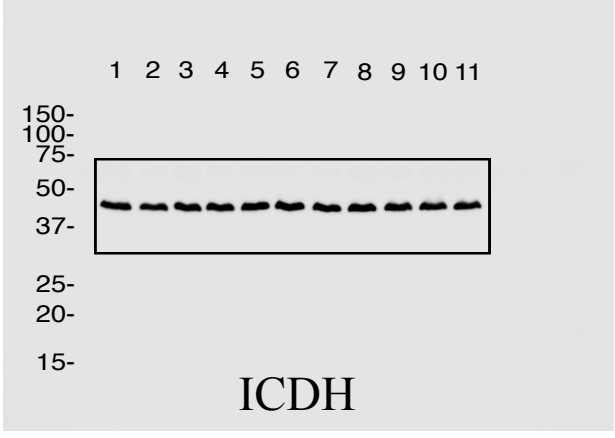

Supplementary Figure 32K. Full length western blots used to generate Supplementary Figure 23. Boxes represent the sections that were used.

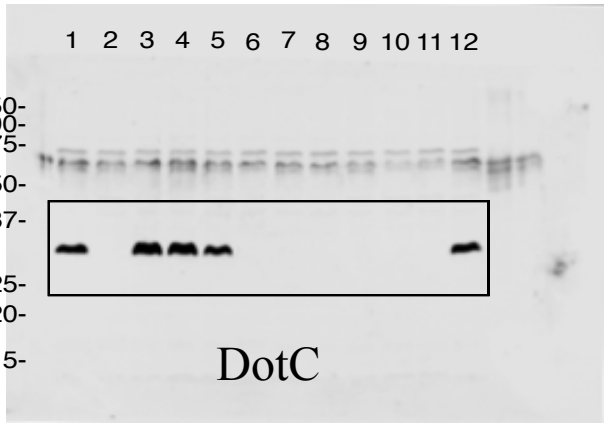

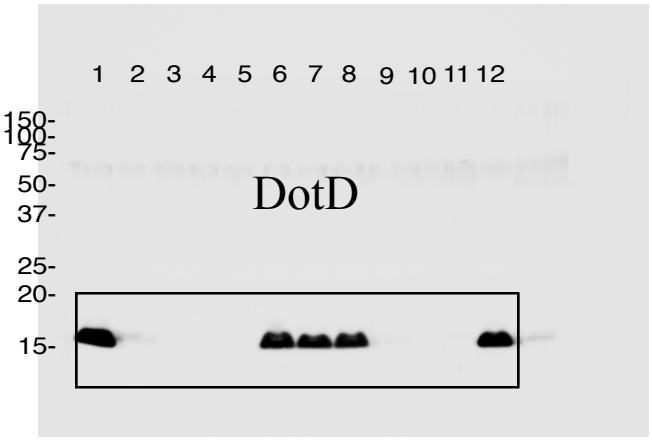

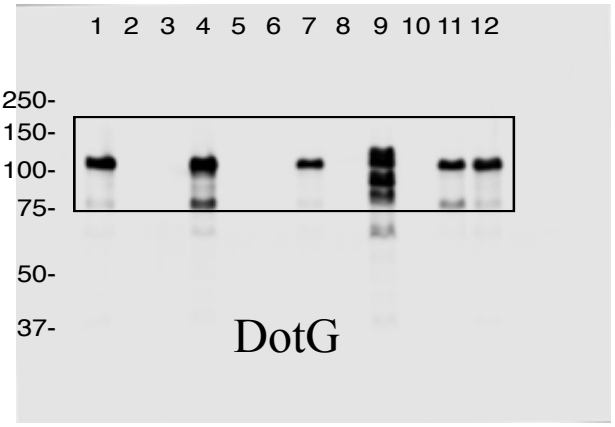

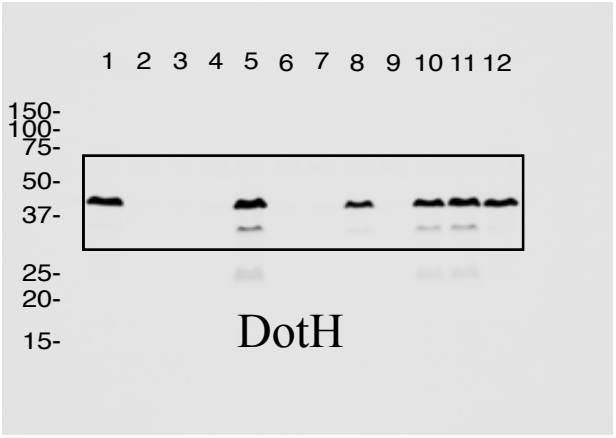

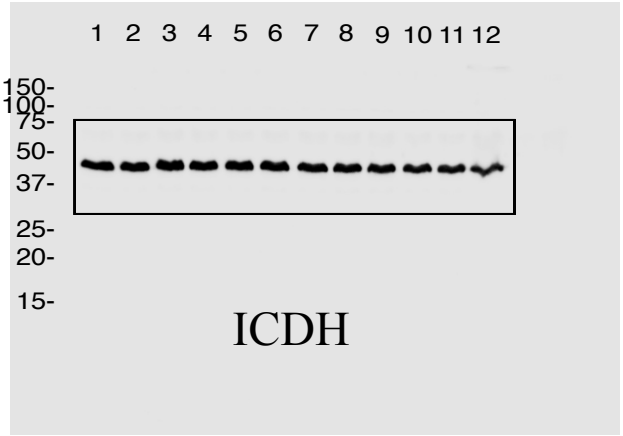

Supplementary Figure 32L. Full length western blots used to generate Supplementary Figure 24. Boxes represent the sections that were used.

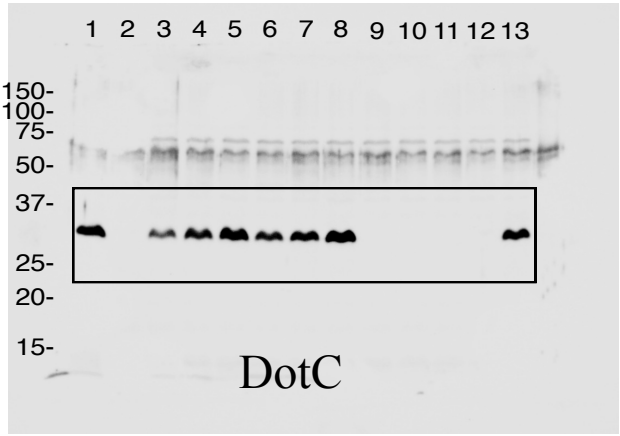

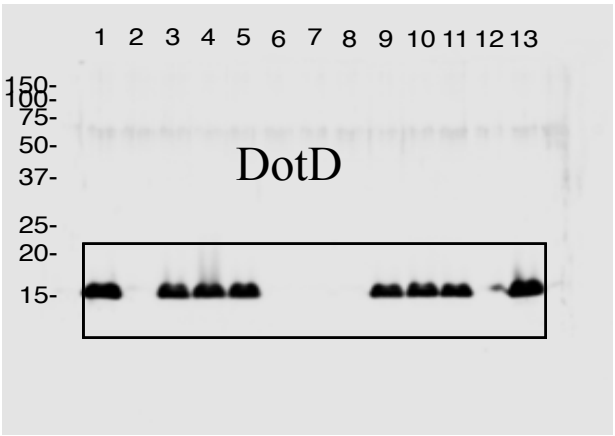

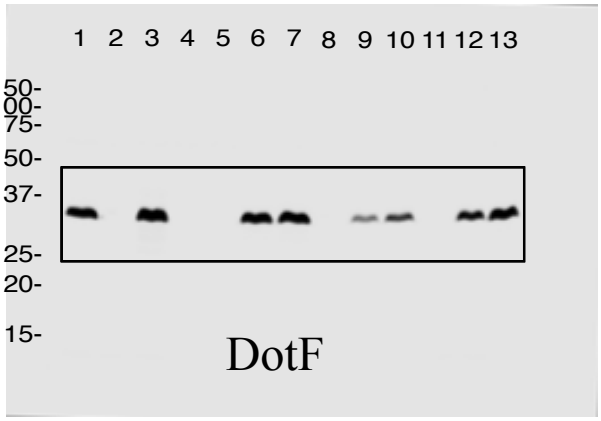

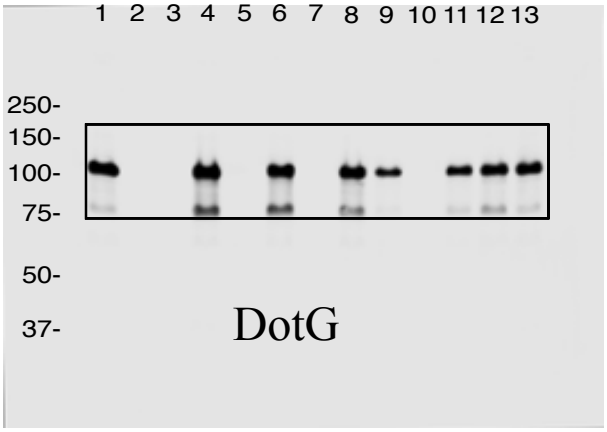

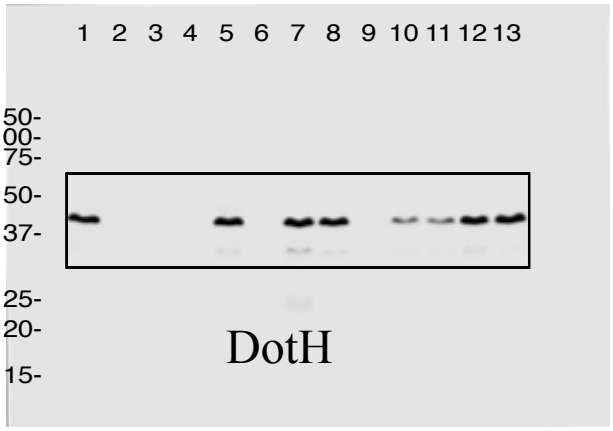

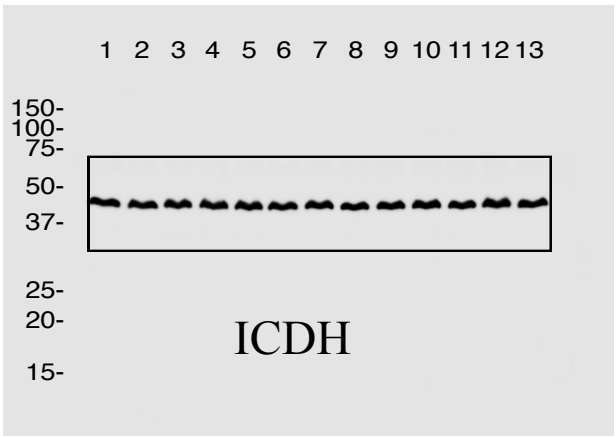

Supplementary Figure 32M. Full length western blots used to generate Supplementary Figure 25. Boxes represent the sections that were used.

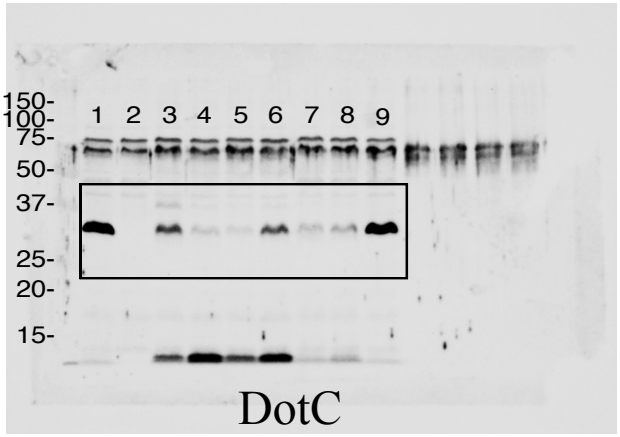

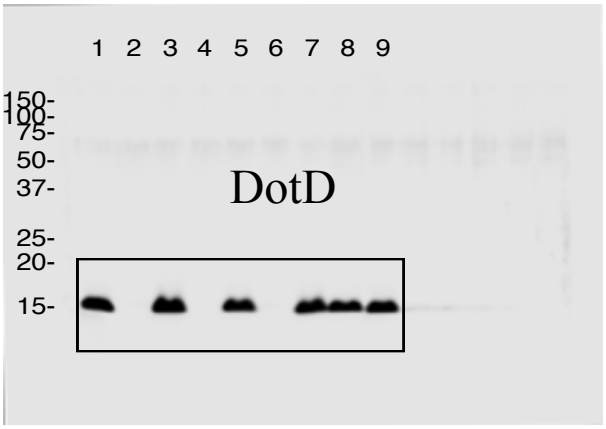

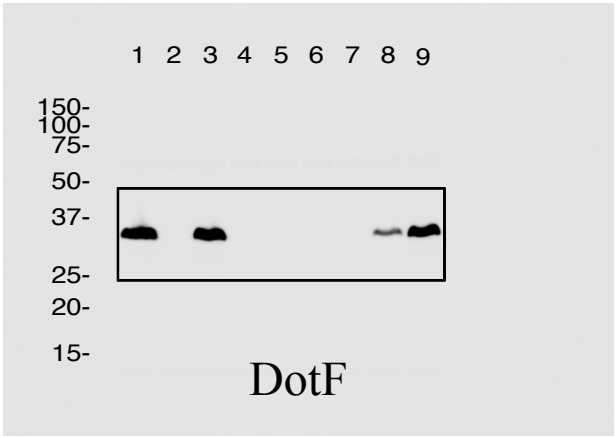

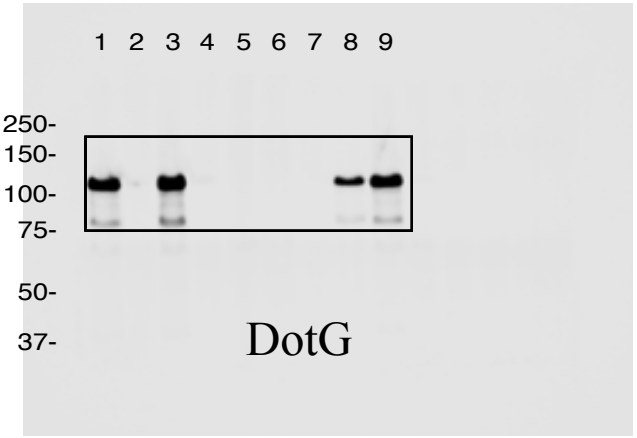

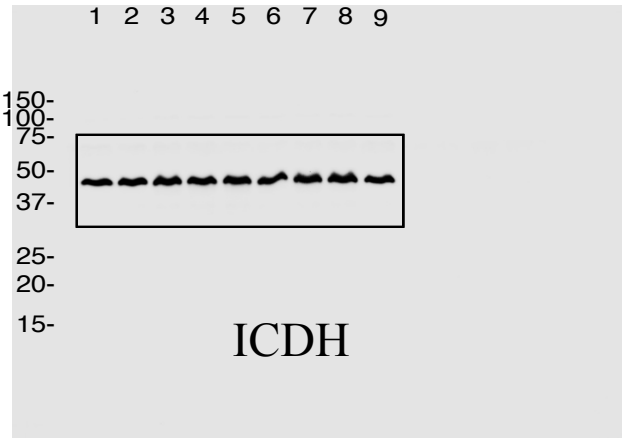

Supplementary Figure 32N. Full length western blots used to generate Supplementary Figure 26. Boxes represent the sections that were used.

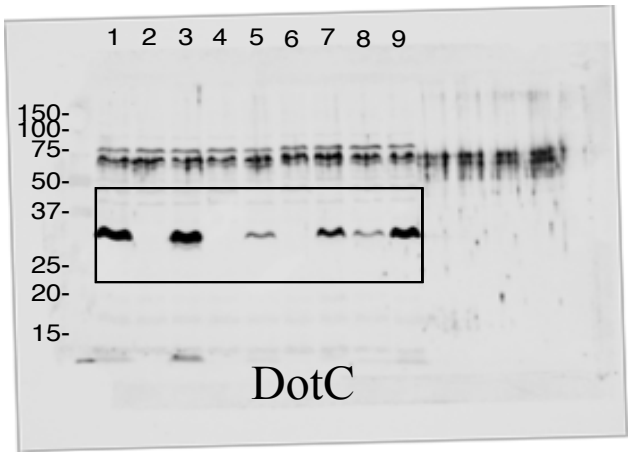

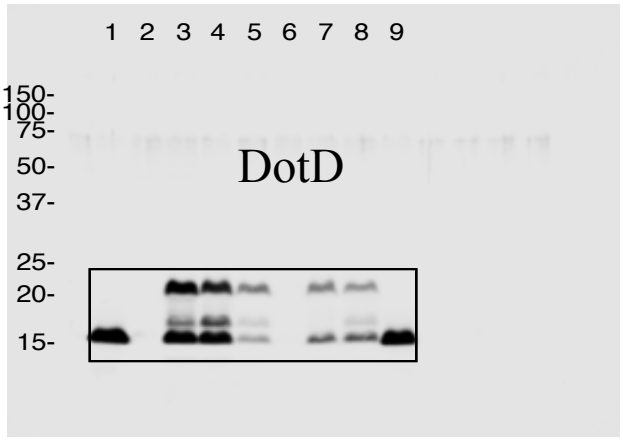

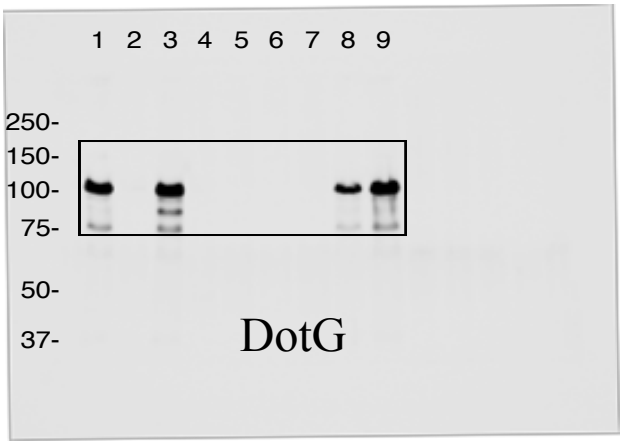

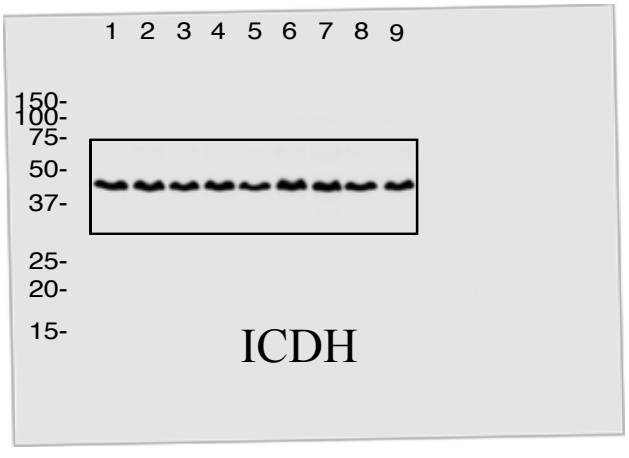

Supplementary Figure 32O. Full length western blots used to generate Supplementary Figure 27. Boxes represent the sections that were used.

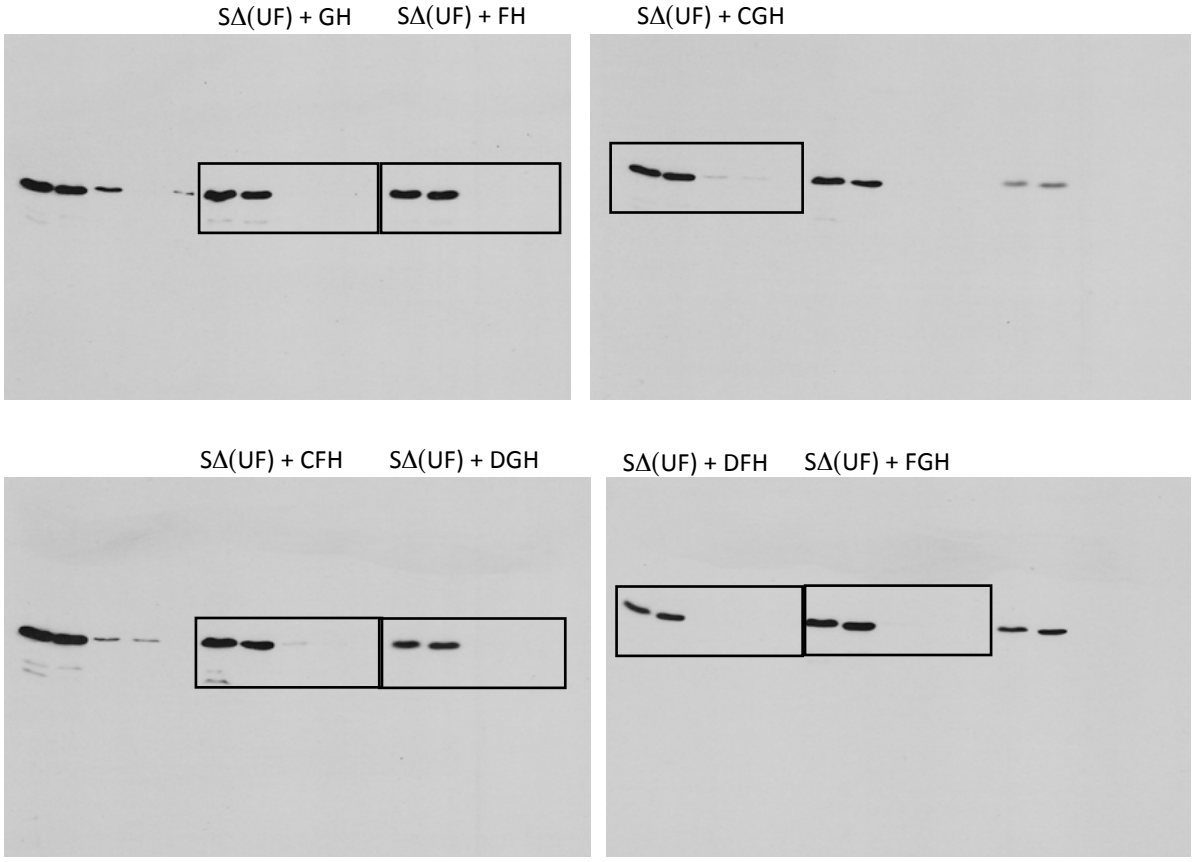

Supplementary Figure 32P. Full length western blots used to generate Fig. 29A. Boxes represent the sections that were used.

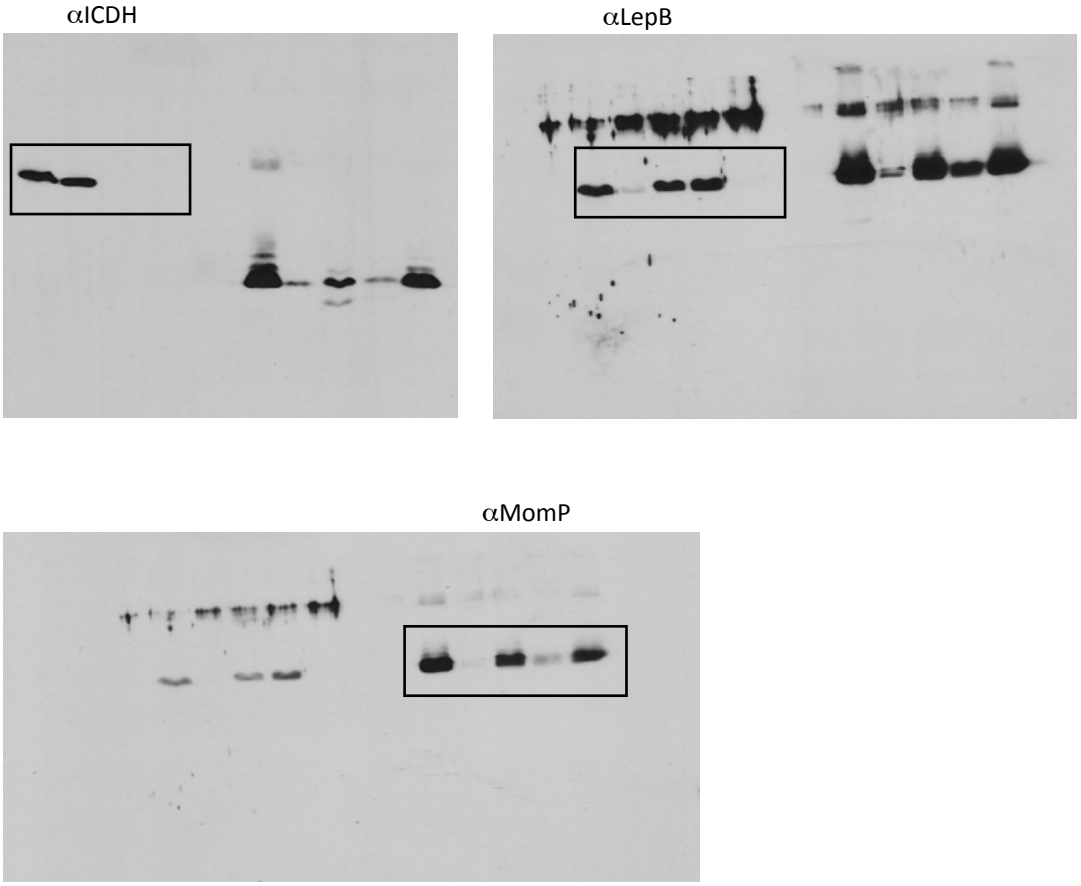

Supplementary Figure 32Q. Full length western blots used to generate Fig. 29B. Boxes represent the sections that were used.

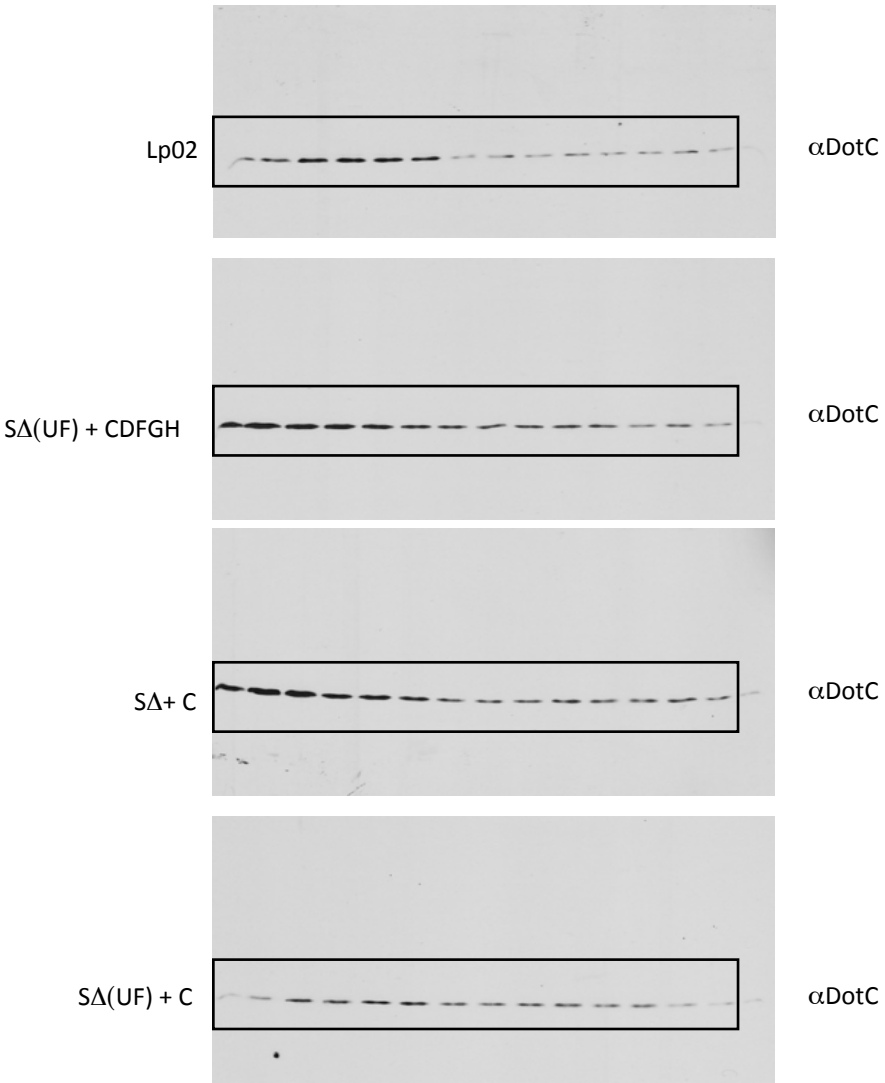

Supplementary Figure 32R. Full length western blots used to generate Fig. 30A. Boxes represent the sections that were used.

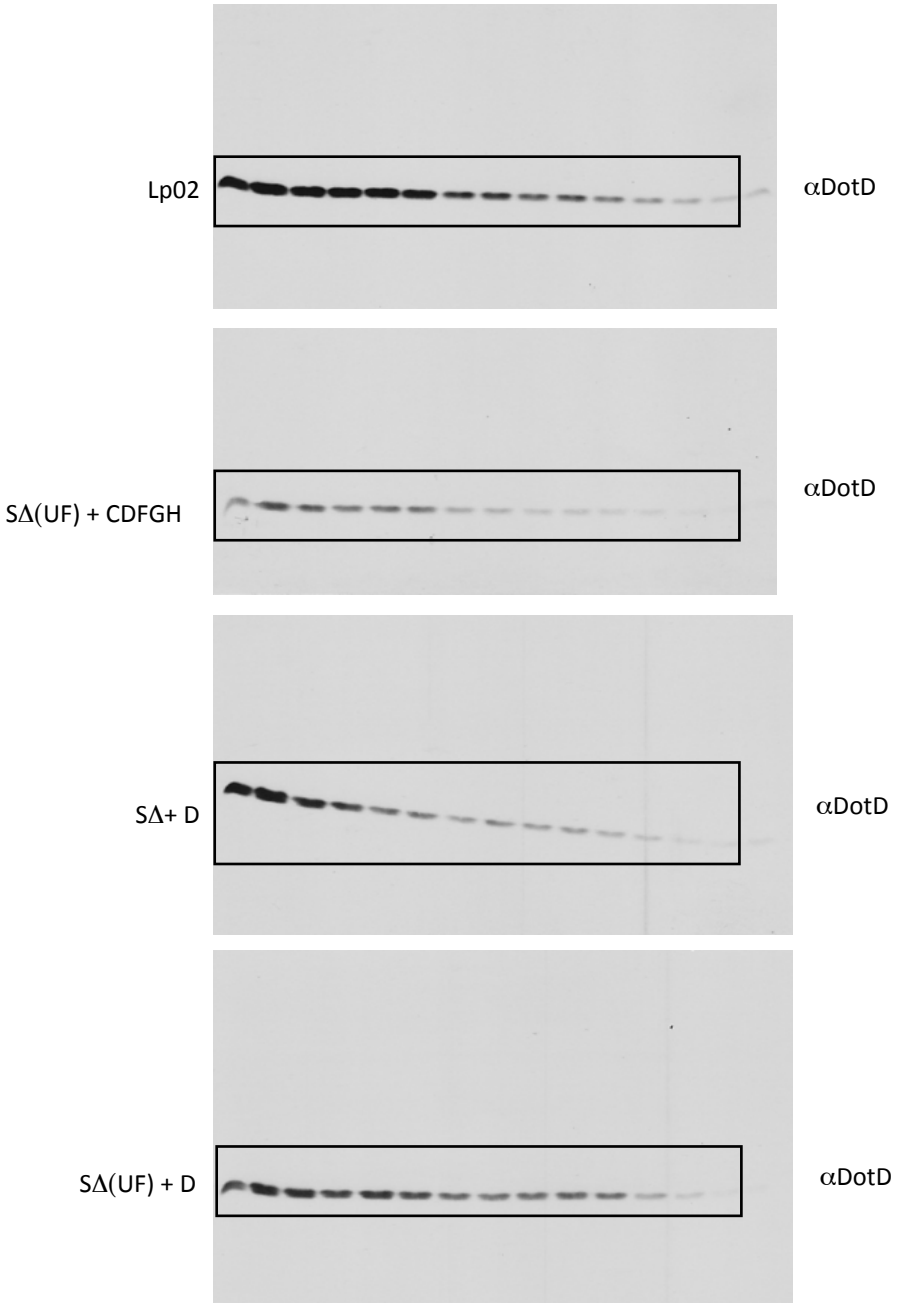

Supplementary Figure 32S. Full length western blots used to generate Fig. 30B. Boxes represent the sections that were used.

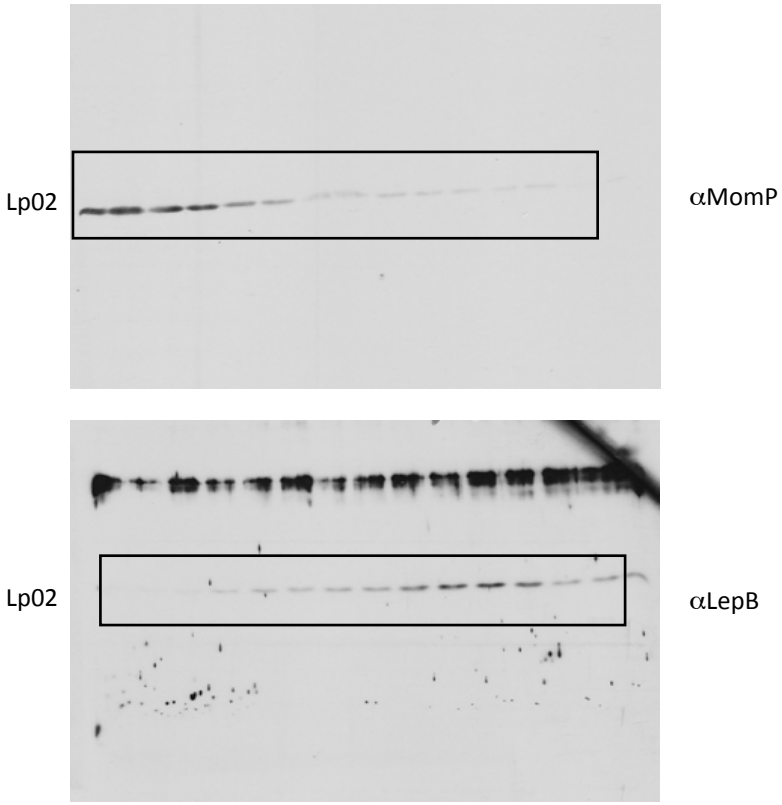

Supplementary Figure 32T. Full length western blots used to generate Fig. 30C. Boxes represent the sections that were used.

Supplementary Movie 1:

Three dimensional representation of the Dot/Icm complex showing windowed secretion chamber (salmon:DotH, grey:DotD, green:DotK and cyan:DotC), wings (yellow:DotF), secretion channel (red:DotG) and top-view of the complex. Cytoplasmic components are not shown. In this 3D representation, IcmF, IcmX and DotA are not visible. Blue structure below the secretion channel represents DotU/IcmF seed that initiates polar Dot/Icm complex assembly.

Supplementary Table 1. Number of tomograms collected and T4SS particles found in different mutants.

No	Strain name	Description	No of tomograms collected	No of particles used for subtomogram averaging
1	Lp02	*Legionella pneumophila thyA* (WT)	188	386
2	JV4044	*Legionella pneumophila thyA Δdot/icm*	80	No particle
3	JV2422	*Legionella pneumophila thyA ΔdotA ΔdotL*	77	195
4	JV3559	*Legionella pneumophila thyA ΔdotG*	164	321
5	JV3563	*Legionella pneumophila thyA ΔdotH*	63	No particle
6	JV3572	*Legionella pneumophila thyA ΔdotD*	121	No particle
7	JV3579	*Legionella pneumophila thyA ΔdotF*	181	212
8	JV3743	*Legionella pneumophila thyA ΔdotC*	65	No particle
9	JV9114	*Legionella pneumophila thyA* DotC-sfGFP	117	375
10	JV6781	*Legionella pneumophila thyA ΔdotL ΔdotO ΔdotB*	109	367
11	JV5443	*Legionella pneumophila* (JV4404 + *dotCDFGH*) + *icmF/dotU*	113	261
12	JV5460	*Legionella pneumophila thyA* (JV4404 + *dotCDH*) + *icmF/dotU*	99	201
13	JV2067	*Legionella pneumophila thyA ΔicmX*	101	309
14	JV3588	*Legionella pneumophila thyA ΔdotK*	107	244
15	JV1180	*Legionella pneumophila thyA ΔdotU ΔicmF*	262	280
16	JV1181	*Legionella pneumophila thyA ΔdotU ΔicmF*	223	378
17	JV9082	*Legionella pneumophila thyA* DotF-sfGFP	75	254

Supplementary Table 2. Bacterial strains and plasmids employed in this study.

Strain, plasmid	Relevant properties	Reference or source
L. pneumophila		
Lp02	Philadelphia-1 *thyA, hsdR, rpsL*	[11]
JV918	Lp02 Δ*dotB*	[12]
JV1179	Lp02 Δ*icmF*	[4]
JV1180	Lp02 Δ*dotU* Δ*icmF*	[3]
JV1181	Lp02 Δ*dotU* Δ*icmF*	[3]
JV1199	Lp02 Δ*dotU* Δ*icmF* + pJB1191 (*dotU icmF*)	[3]
JV1571	Lp02 Δ*dotV*	[4]
JV1644	Lp02 Δ*dotO*	[4]
JV1648	Lp02 Δ*dotP*	[4]
JV1928	Lp02 Δ*icmQ*	[4]
JV1951	Lp02 Δ*icmR*	[4]
JV1962	Lp02 Δ*icmS*	[4]
JV2064	Lp02 Δ*dotA*	[4]
JV2067	Lp02 Δ*icmX*	[4]
JV2422	Lp02 Δ*dotA* Δ*dotL*	[13]
JV2725	Lp02 Δ*dotE*	[4]
JV2841	Lp02 Δ*lvgA*	[5]
JV3559	Lp02 Δ*dotG*	[4]
JV3563	Lp02 Δ*dotH*	[4]
JV3566	Lp02 Δ*icmT*	[4]
JV3572	Lp02 Δ*dotD*	[4]
JV3579	Lp02 Δ*dotF*	[4]
JV3588	Lp02 Δ*dotK*	[4]
JV3590	Lp02 Δ*dotJ*	[4]
JV3596	Lp02 Δ*dotI*	[4]
JV3598	Lp02 Δ*icmW*	[4]
JV3709	Lp02 Δ*icmV*	[4]
JV3719	Lp02 Δ*dotA* Δ*dotN*	[4]
JV3743	Lp02 Δ*dotC*	[4]
JV4015	Lp02 Δ*dotU*	[4]
JV4044	Lp02 super *dot/icm* deletion Δ*dotU* Δ*icmF lvgA+*	
JV4668	JV4044 + pJB1554 (*dotG*)	This study
JV4669	JV4044 + pJB2121 (*dotF*)	This study
JV4671	JV4044 + pJB1555 (*dotH*)	This study
JV4694	JV4044 + pJB4225 (*dotC:HA3X)*	This study
JV4695	JV4044 + pJB4223 (*dotD:HA3X*)	This study
JV5263	Δ*dotC* + pJB1625 (vector)	This study
JV5264	Δ*dotC* + pJB4202 (*dotC* complementing clone)	This study
JV5266	Δ*dotD* + pJB1625 (vector)	This study
JV5267	Δ*dotD* + pJB4204 (*dotD* complementing clone)	This study
JV5268	Δ*dotD* + pJB4223 (*dotD:HA3X*)	This study
JV5319	Lp02 super *dot/icm* deletion *dotU+ icmF+ lvgA+*	[4]
JV5361	Lp02 Δ*dotA* Δ*dotM*	[4]

JV5403	JV5319 + pJB2121 (*dotF*)	This study
JV5404	JV5319 + pJB1554 (*dotG*)	This study
JV5405	JV5319 + pJB1555 (*dotH*)	This study
JV5406	JV5319 + pJB4005 (*dotGH*)	This study
JV5407	JV5319 + pJB2123 (*dotFH*)	This study
JV5408	JV5319 + pJB4263 (*dotFG*)	This study
JV5409	JV5319 + pJB4006 (*dotFGH*)	This study
JV5439	JV5319 + pJB4025 (*dotCFGH*)	This study
JV5441	JV5319 + pJB4026 (*dotDFGH*)	This study
JV5442	JV4044 + pJB4027 (*dotCDFGH*)	This study
JV5443	JV5319 + pJB4027 (*dotCDFGH*)	[14]
JV5452	JV5319 + pJB4409 (*dotCF*)	This study
JV5453	JV5319 + pJB4410 (*dotDF*)	This study
JV5454	JV5319 + pJB4411 (*dotCDF*)	This study
JV5455	JV5319 + pJB4412 (*dotCG*)	This study
JV5456	JV5319 + pJB4413 (*dotDG)*	This study
JV5457	JV5319 + pJB4414 (*dotCDG*)	This study
JV5458	JV5319 + pJB4415 (*dotCH*)	This study
JV5459	JV5319 + pJB4416 (*dotDH)*	This study
JV5460	JV5319 + pJB4417 (*dotCDH*)	This study
JV5464	JV5319 + pJB4419 (*dotCFH*)	This study
JV5465	JV5319 + pJB4421 (*dotDFH*)	This study
JV5466	JV5319 + pJB4422 (*dotCDFH*)	This study
JV5467	JV5319 + pJB4420 (*dotCFG*)	This study
JV5468	JV5319 + pJB4423 (*dotCDFG*)	This study
JV5469	JV5319 + pJB4019 (*dotC*)	This study
JV5470	JV5319 + pJB4021 (*dotD*)	This study
JV5471	JV5319 + pJB4023 (*dotCD*)	This study
JV5472	JV5319 + pJB4425 (*dotDFG*)	This study
JV5473	JV5319 + pJB4029 (*dotCGH*)	This study
JV5474	JV5319 + pJB4031 (*dotDGH*)	This study
JV5475	JV5319 + pJB4033 (*dotCDGH*)	This study
JV5480	JV5319 + pJB4225 (*dotC:HA3X)*	This study
JV5481	JV5319 + pJB4223 (*dotD:HA3X*)	This study
JV5482	JV5319 + pJB4546 (*dotC:HA3X dotD*)	This study
JV5483	JV5319 + pJB4547 (*dotC dotD:HA3X*)	This study
JV5484	Δ*dotC* + pJB4542 (*dotC:HA3X)*	This study
JV5486	JV5319 + pJB4550 (*dotD:HA3X dotH)*	This study
JV5749	JV5319 + pJB4555 (*dotC:HA3X dotH)*	This study
JV5750	JV5319 + pJB4556 (*dotC:HA3X dotD dotH*)	This study
JV5751	JV5319 + pJB4557 (*dotC dotD:HA3X dotH*)	This study
JV5752	JV5319 + pJB4558 (*dotC:HA3X dotD dotFGH)*	This study
JV5753	JV5319 + pJB4559 (*dotC dotD:HA3X dotFGH)*	This study
JV6781	Lp02 Δ*dotL* Δ*dotO* Δ*dotB*	This study
JV7967	Lp02 Δ*dotI* Δ*dotJ*	This study
JV7058	Lp02 Δ*dotH* Δ*dotG* Δ*dotF*	This study
JV7091	Lp02 Δ*dotE* Δ*dotP*	This study
JV9082	Lp02 DotF-sfGFP integrated on chromosome	This study
JV9114	Lp02 DotC-sfGFP integrated on chromosome	This study

Plasmids

pJB908	RSF1010 cloning vector	[12]
pJB1001	Δ*dotL* suicide plasmid	[13]
pJB1333	Δ*dotO* suicide plasmid	[4]
pJB1554	pJB908 with *dotG*	[3]
pJB1555	pJB908 with *dotH*	[3]
pJB2121	pJB908 with *dotF*	[3]
pJB2123	pJB908 with *dotFH*	This study
pJB4005	pJB908 with *dotGH*	This study
pJB4006	pJB908 with *dotFGH*	This study
pJB4019	pJB908 with *dotC*	This study
pJB4021	pJB908 with *dotD*	This study
pJB4023	pJB908 with *dotCD*	This study
pJB4025	pJB908 with *dotCFGH*	This study
pJB4026	pJB908 with *dotDFGH*	This study
pJB4027	pJB908 with *dotCDFGH*	This study
pJB4029	pJB908 with *dotCGH*	This study
pJB4031	pJB908 with *dotDGH*	This study
pJB4033	pJB908 with *dotCDGH*	This study
pJB4223	pJB908 with *dotD:HA3X*	This study
pJB4225	pJB908 with *dotC:HA3X*	This study
pJB4263	pJB908 with *dotFG*	This study
pJB4409	pJB908 with *dotCF*	This study
pJB4410	pJB908 with *dotDF*	This study
pJB4411	pJB908 with *dotCDF*	This study
pJB4412	pJB908 with *dotCG*	This study
pJB4413	pJB908 with *dotDG*	This study
pJB4414	pJB908 with *dotCDG*	This study
pJB4415	pJB908 with *dotCH*	This study
pJB4416	pJB908 with *dotDH*	This study
pJB4417	pJB908 with *dotCDH*	This study
pJB4419	pJB908 with *dotCFH*	This study
pJB4420	pJB908 with *dotCFG*	This study
pJB4421	pJB908 with *dotDFH*	This study
pJB4422	pJB908 with *dotCDFH*	This study
pJB4423	pJB908 with *dotCDFG*	This study
pJB4425	pJB908 with *dotDFG*	This study
pJB4546	pJB908 with *dotC:HA3X dotD*	This study
pJB4547	pJB908 with *dotC dotD:HA3X*	This study
pJB4550	pJB908 with *dotD:HA3X dotH*	This study
pJB4555	pJB908 with *dotC:HA3X dotH*	This study
pJB4556	pJB908 with *dotC:HA3X dotD dotH*	This study
pJB4557	pJB908 with *dotC dotD:HA3X dotH*	This study
pJB4558	pJB908 with *dotC:HA3X dotD dotFGH*	This study
pJB4559	pJB908 with *dotC dotD:HA3X dotFGH*	This study
pJB5184	Δ*dotH* Δ*dotG* Δ*dotF* suicide plasmid	This study
pJB5185	Δ*dotE* Δ*dotP* suicide plasmid	This study
pJB6162	Δ*dotJ* Δ*dotI* suicide plasmid	This study

pJB7255	DotF-sfGFP integration plasmid	This study
pJB7264	DotC-sfGFP with SacB/CmR cassette	This study
pJB7283	DotC-sfGFP integration plasmid	This study
pSR47S	R6K suicide vector	[15]

Supplementary References

1 Kucukelbir, A., Sigworth, F. J. & Tagare, H. D. Quantifying the local resolution of cryo-EM density maps. *Nat Methods* **11**, 63-65, doi:10.1038/nmeth.2727 (2014).

2 Jeong, K. C., Ghosal, D., Chang, Y.-W., Jensen, G. J. & Vogel, J. P. Polar delivery of *Legionella* type IV secretion system substrates is essential for virulence. *Proceedings of the National Academy of Sciences* **114**, 8077-8082, doi:10.1073/pnas.1621438114 (2017).

3 Sexton, J. A., Miller, J. L., Yoneda, A., Kehl-Fie, T. E. & Vogel, J. P. *Legionella pneumophila* DotU and IcmF are required for stability of the Dot/Icm complex. *Infect Immun* **72**, 5983-5992 (2004).

4 Vincent, C. D. *et al.* Identification of the core transmembrane complex of the *Legionella* Dot/Icm type IV secretion system. *Mol Microbiol* **62**, 1278-1291 (2006).

5 Vincent, C. D. & Vogel, J. P. The *Legionella pneumophila* IcmS-LvgA protein complex is important for Dot/Icm-dependent intracellular growth. *Mol Microbiol* **61**, 596-613, doi:10.1111/j.1365-2958.2006.05243.x (2006).

6 Kelley, L. A., Mezulis, S., Yates, C. M., Wass, M. N. & Sternberg, M. J. E. The Phyre2 web portal for protein modeling, prediction and analysis. *Nature Protocols* **10**, 845-858, doi:10.1038/nprot.2015.053 (2015).

7 Yang, J. *et al.* The I-TASSER Suite: protein structure and function prediction. *Nature Methods* **12**, 7-8, doi:10.1038/nmeth.3213 (2015).

8 Xu, D. & Zhang, Y. Ab initio protein structure assembly using continuous structure fragments and optimized knowledge-based force field. *Proteins* **80**, 1715-1735, doi:10.1002/prot.24065 (2012).

9 Low, H. H. *et al.* Structure of a type IV secretion system. *Nature* **508**, 550-553, doi:10.1038/nature13081 (2014).

10 Chetrit, D., Hu, B., Christie, P. J., Roy, C. R. & Liu, J. A unique cytoplasmic ATPase complex defines the *Legionella pneumophila* type IV secretion channel. *Nat Micro*, doi:doi:10.1038/s41564-018-0165-z (2018).

11 Berger, K. H. & Isberg, R. R. Two distinct defects in intracellular growth complemented by a single genetic locus in *Legionella pneumophila*. *Mol Microbiol* **7**, 7-19 (1993).

12 Sexton, J. A. *et al.* The *Legionella pneumophila* PilT homologue DotB exhibits ATPase activity that is critical for intracellular growth. *J Bacteriol* **186**, 1658-1666 (2004).

13 Buscher, B. A. *et al.* The DotL protein, a member of the TraG-coupling protein family, is essential for viability of *Legionella pneumophila* strain Lp02. *J Bacteriol* **187**, 2927-2938, doi:10.1128/JB.187.9.2927-2938.2005 (2005).

14 Ghosal, D., Chang, Y. W., Jeong, K. C., Vogel, J. P. & Jensen, G. J. In situ structure of the *Legionella* Dot/Icm type IV secretion system by electron cryotomography. *EMBO Rep* **18**, 726-732, doi:10.15252/embr.201643598 (2017).

15 Merriam, J. J., Mathur, R., Maxfield-Boumil, R. & Isberg, R. R. Analysis of the *Legionella pneumophila fliI* gene: intracellular growth of a defined mutant defective for flagellum biosynthesis. *Infect Immun* **65**, 2497-2501 (1997).